Early events in copper-ion catalyzed oxidation of α-synuclein

Manish K. Tiwari[a]; Fabian Leinisch[b], Cagla Sahin[c], Ian Max Møller[d], Daniel E. Otzen[c]; Michael J. Davies[b] and Morten J. Bjerrum[a] *

[a] *Department of Chemistry, University of Copenhagen, Copenhagen, Denmark*

[b] *Department of Biomedical Sciences, University of Copenhagen, Copenhagen, Denmark*

[c] *Department of Molecular Biology and Genetics, Aarhus University, Aarhus C, Denmark*

[d] *Department of Molecular Biology and Genetics, Aarhus University, Slagelse, Denmark*

Running title: Copper-ion catalyzed oxidation of α-synuclein

Abbreviations used: α–SN, α–synuclein; PD, Parkinson's disease; Met, methionine; Tyr, tyrosine; His, histidine, $AscH^-$, ascorbate; 2Na–EDTA, Ethylenediaminetetraacetic acid disodium salt; MOPS, 3–(N–morpholino) propane–sulfonic acid.

**Corresponding author at:* Department of Chemistry, University of Copenhagen,

Universitetsparken 5, DK–2100 Copenhagen, Denmark

Email address: mobj@chem.ku.dk (M. J. Bjerrum)

Running title: Copper-ion catalyzed oxidation of α-synuclein

HIGHLIGHTS

- Met and Tyr oxidation are early and rapid events in Cu^{2+}/H_2O_2– mediated damage to α–synuclein.
- Met sulfoxide and dityrosine detected within 5 min of Cu^{2+}/H_2O_2 exposure to α–synuclein.
- Carbonyl formation is a minor process in early Cu^{2+}/H_2O_2– mediated damage to α–synuclein.
- Ascorbate limits Met and Tyr oxidation in Cu^{2+}/H_2O_2 /$AscH^-$–mediated damage to α–synuclein.

GRAPHICAL ABSTRACT

ABSTRACT

Previous studies on metal–ion catalyzed oxidation of α–synuclein oxidation have mostly used conditions that result in extensive modification precluding an understanding of the early events in this process. In this study, we have examined time-dependent oxidative events related to α–synuclein modification using six different molar ratios of Cu^{2+}/H_2O_2/protein and Cu^{2+}/H_2O_2/ascorbate/protein resulting in mild to moderate extents of oxidation. For a Cu^{2+}/H_2O_2/protein molar ratio of 2.3:7.8:1 only low levels of carbonyls were detected (0.078 carbonyls per protein), whereas a molar ratio of 4.7:15.6:1 gave 0.22 carbonyls per α–synuclein within 15 min. With the latter conditions, rapid conversion of 3 out of 4 methionines (Met) to methionine sulfoxide, and 2 out of 4 tyrosines (Tyr) were converted to products including inter– and intra–molecular dityrosine cross-links and protein oligomers, as determined by SDS–PAGE and Western blot analysis. Limited histidine (His) modification was observed. The rapid formation of dityrosine cross-links was confirmed by fluorescence and mass–spectrometry. These data indicate that Met and Tyr oxidation are early events in Cu^{2+}/H_2O_2-mediated damage, with carbonyl formation being a minor process. With the Cu^{2+}/H_2O_2/ascorbate system, rapid protein carbonyl formation was detected with the first 5 min, but after this time point, little additional carbonyl formation was detected. With this system, lower levels of Met and Tyr oxidation were detected (2 Met and 1 Tyr modified with a Cu^{2+}/H_2O_2/ascorbate/protein ratio of 2.3:7.8:7.8:1), but greater His oxidation. Only low levels of intra– dityrosine cross-links and no inter– dityrosine oligomers were detected under these conditions, suggesting that ascorbate limits Cu^{2+}/H_2O_2-induced α–synuclein modification.

Keywords: α–Synuclein, Metal-catalyzed oxidation, Oxidative stress, Parkinson's disease, Dityrosine, Methionine sulfoxide, Protein carbonyls, Cross–links.

1. Introduction

One-electron reduction of O_2 by electron–transfer chains of mitochondria gives rise to superoxide anion ($O_2^{\bullet-}$) and subsequently hydrogen peroxide (H_2O_2) [1, 2]. Further reactions of these species can generate the hydroxyl radical ($^{\bullet}OH$), as well as non-radical species such as singlet oxygen ($^1O_2$). The formation and subsequent reactions of these species are therefore a significant feature of aerobic life [3, 4]. Excessive production of these species, and/or impaired antioxidant defense mechanisms, can give rise to increased oxidative stress in cellular systems [5] and has been implicated in various pathological conditions including Parkinson's disease (PD) [6], Alzheimer's disease (AD) [7, 8], Amyotrophic Lateral Sclerosis (ALS) [9], Huntington disease (HD) [10] and Prion diseases [11] leading to neurodegeneration and cell death [1].

PD, the second most prevalent neurodegenerative disease after AD [12], is characterized by gradual impairment of physical abilities due to severe loss of dopaminergic neurons in the *substantia nigra* region of the brain of PD patients [13]. PD mostly occurs sporadically, but genetically inherited PD accounts for ~15% of all cases [14]. A central hallmark of PD is the intraneuronal aggregation of the protein α-synuclein (α-SN) into amyloid-rich Lewy bodies [15, 16]. α-SN is a 140 amino acid presynaptic protein [17] with a relatively undefined regulatory function, though it is believed to be involved in synaptic regulation [18]. Native α–SN consists of three distinct domains: a lipid-binding N–terminal region (residues 1 – 60), a hydrophobic self-aggregating non–amyloid β component (residues 61 – 95), and an acidic C-terminal region (residues 96 − 140) that prevents rapid filament assembly [19]. A clear correlation between the formation of intracellular oligomeric species of α-SN within the *substantia nigra* and PD has been reported, and it has been suggested that transient partially-folded α–SN species are key to fibrillization [20]. Although it is unclear how α–SN triggers neuronal death [21] and aggregation

of α–SN has been attributed to complex processes, oxidatively generated damage appears to be a major risk factor [22, 23]. Oxidized forms of methionine (Met) [24] and tyrosine (Tyr) [25, 26] have been shown to be abundant in Lewy body deposits [26], consistent with a role for oxidative stress in PD [1, 2]. Elevated levels of Fe ions [27, 28] in the *substantia nigra* and altered Cu ion concentrations [29] have been reported in PD brains, and evidence has been presented that dysregulated metal ion (iron, copper, and zinc) homeostasis is directly linked to the pathological processes of protein aggregation and oxidatively generated damage in PD and other neurodegenerative conditions [2, 30]. In vitro studies have suggested that fibrillation of α–SN is promoted by metal ions [31], with Cu^{2+} the most effective [32]. Moreover, Cu^{2+} accelerates aggregation of α–SN *in vitro*, via oxidation of C–terminal residues [32]. However, the early molecular events leading to the transient conversion of unstructured monomeric α–SN into oligomers and fibrils have yet to be defined.

Several structural and dynamic studies [33, 34] have focused on elucidating Cu^{2+} coordination and structural determinants of Cu^{2+} binding to α–SN [32, 35-37], and the role of metal ion–catalyzed oxidation (MCO) on α–SN aggregation/oligomerization [24, 26, 31, 38-41]. These studies have used Cu^{2+} concentrations in the range 500 µM – 5000 µM, with 300 – 1250 µM H_2O_2 and 100 pmol – 37 µM α–SN, resulting in high metal–ion : protein ratios (13 – 130 fold), and high H_2O_2 : protein ratios (8-34 fold) [26, 31, 38-40], with this resulting in extensive oxidation. Furthermore, many studies have used long incubation periods (16 – 24 h) [26, 38], and buffers that contain phosphate [38, 41] or Tris [31, 39], which can act as metal ion chelators [42]. These studies are summarized in Table S1. Although these studies have confirmed that metal ions, such as Cu^{2+} can catalyze oxidation of PD, the relationship between the early events of α–SN oxidation, and the chemical and structural changes that may lead to aggregation are still unclear.

The aim of the present study was, therefore, to systematically investigate: i) the effects of low to moderate levels of Cu^{2+}, H_2O_2, and $AscH^-$ on α–SN at physiological pH values and short reaction times; and ii) to evaluate the structural and chemical changes that occur on the α–SN. The resulting data may help elucidate the early alternations of α–SN that are involved in the initiation of PD.

2. Materials and methods

2.1. Materials

Expression and purification of full–length recombinant human α–SN (residues 1–140) were achieved as described previously [43]. Stabilizer–free 30% hydrogen peroxide (H_2O_2) and copper (II) chloride dihydrate ($CuCl_2 \times 2H_2O$) was supplied by Merck Chemicals GmbH (Darmstadt, Germany). Ethylenediaminetetraacetic acid disodium salt (2Na–EDTA) and 3–(N–morpholino) propane–sulfonic acid (MOPS) were obtained from BDH Ltd. (Poole, England). L–Ascorbic acid was supplied by Sigma–Aldrich (St. Louis, MO, USA). All chemicals and reagents were obtained with highest purity grade (>99.5%).

2.2. Preparation of Buffer, Chemicals, and α–Synuclein Solutions

Stock solutions of $CuCl_2$ (10 mM), H_2O_2 (10 mM) and EDTA (40 mM) was prepared using Milli–Q water. The concentration of the H_2O_2 stock solution was quantified by UV–Vis absorbance (Milli–Qwater as blank) at 265 nm using ε 10 M^{-1} cm^{-1} [44]. Milli–Q water, buffer, α–SN and chemical solutions were filtered using a 0.2 µm filter before use. Purified wild-type α–SN was dissolved in freshly–prepared 20 mM MOPS–NaOH buffer (pH 7.4) and the

concentration determined from its UV absorbance (Agilent UV–visible ChemStation) at 280 nm using an extinction coefficient of 5960 M^{-1} cm^{-1}[45].

2.3. Cu^{2+}–mediated oxidation of α–SN

A constant concentration of α–SN (57.6 μM) was employed with the final concentrations of the oxidant systems being as follows: Cu^{2+} (135 – 270 μM), H_2O_2 (450 – 900 μM) and $AscH^-$ (450 – 900 μM), with six combinations of these examined (hereafter defined as condition 1– 6; see Table 1). The components were mixed at room temperature (22 ºC) and a sample aliquot was removed and quenched immediately after mixing with EDTA (< 8 s) and placed on ice. This sample is defined as the 0.1 min incubation time point. The remaining material was transferred to a 37 ºC heating block, and further aliquots withdrawn at 5, 15, 30, 60, 180 and 360 min of incubation. Immediately after sampling the reactions were quenched with 2 mM EDTA, a concentration shown in pilot studies to prevent further oxidation. Control samples were also prepared at the 0.1 and 360 min time points, each with one component of the reaction system. Samples were aliquoted into separate tubes and flash frozen in liquid N_2 and stored at –80 ºC for further analysis.

2.4. Determination of α–SN integrity by capillary electrophoresis

Capillary electrophoresis (CE) was performed on a temperature–controlled Hewlett–Packard 3DCE (Agilent) equipped with UV–Vis diode array detector operating between 200 – 600 nm. Separation was performed using a 75 cm x 0.005 cm fused silica capillary, with the pH,

ionic strength of the buffer and the voltage adapted to avoid any modification in the α–SN charge distribution as well as Joule effect. The temperature of capillary cassette was 25 °C, the vial holder temperature 15 °C, the voltage 25 kV with a typical current of 55 µA. The separation buffer consisted of 50 mM Na phosphoric acid at pH 2.1. The capillary was rinsed with 1 M NaOH for 10 min followed by 10 min with the Milli–Q water at 930 mbar. Prior to each run, the capillary was rinsed with 0.1 M NaOH followed by the separation buffer for 3 min each. All samples were injected at 50 mbar for 10 s, with the capillary then plugged by injecting separation buffer under the same conditions. On–column detection was at 220 nm. Instrument control and data acquisition were performed using ChemStation software (Agilent Technologies).

2.5. Detection and quantification of protein carbonyls

Protein carbonyl quantification was carried using the OxiSelect™ protein carbonyl fluorometric [46] assay kit (Cell Biolabs, San Diego, CA, USA) as described by the manufacturer, except with minor modifications to the washing and dilution steps. Briefly, 50 µL of each sample was mixed with the supplied fluorophore reagent and incubated for ~16 h in darkness at 22 °C. The samples were then precipitated with 400 µL of cold trichloroacetic acid (TCA) and unbound fluorophore removed by three washes with 1 mL cold acetone, each followed by centrifugation at 10000 g for 15 min at 4 °C. After evaporating residual acetone, the pellets were solubilized using 50 µL of the guanidinium chloride (GuHCl) provided with the kit and incubated at 22 °C. The dissolved pellets were diluted 6-fold by adding 250 µL of assay diluent and then centrifuged for 15 min at 4 °C at 10000 g. Samples and standards (100 µL), in duplicate, were placed into clear bottomed 96–well black fluorescence microtiter plate (Thermo Scientific Nunc, Thermo Fisher) and fluorescence spectra recorded (λ_{ex} 485 nm, λ_{em} 530 nm)

using a Molecular Devices SpectraMax M2 instrument (Sunnyvale, CA, USA). The supplied fluorophore standard was used to generate a standard curve in each assay run and the equation obtained from the standard curve was used to calculate the carbonyl concentration in each sample. With the exception of the incubations, all steps were undertaken at 4 °C. Aliquots were also taken prior to carbonyl quantification, for assessment of protein concentration using the BCA assay [47]. Data are presented as the number of carbonyls per α–SN molecule.

2.6. Examination of α–SN structure by circular dichroism

Far–UV (178 − 260 nm) CD spectra of α–SN samples were collected at 25 °C on a Jasco J–815 spectropolarimeter equipped with a Peltier–element–controlled thermostat, using a spectral bandwidth of 2 nm, a digital integration time of 4 s, a scanning speed of 20 nm min^{-1}, and a 0.005–cm path length cell. Blank spectra of the sample buffer (20 mM MOPS–NaOH buffer, pH 7.4) were subtracted from the mean spectrum of three individual scans, using the Jasco Spectra Analysis software, and a Savitzky–Golay algorithm (of convolution width 11) applied.

2.7. Amino acid analysis of α–SN samples

Amino acid hydrolysis was carried out as described previously [48]. Hydrolyzed samples were analyzed by UPLC using a Shimadzu Nexera system with an SIL–30AC autosampler (set at 4 °C) and a RF–20A fluorescence detector set with λ_{ex} 340 nm, λ_{em} 440 nm. Data analysis was carried out using Shimadzu Lab Solutions Browser. Retention times and concentrations were assigned by comparison to commercial amino acid standards, and data were normalized to the alanine (Ala) content to compensate for any losses during processing [48].

2.8. SDS–PAGE analysis of α–SN samples

Samples were analyzed by SDS–PAGE to examine changes in protein integrity under reducing conditions. Samples and molecular mass markers (Invitrogen pre-stained marker 161–036) were electrophoresed on 4–12% NuPAGE Bis-Tris mini acrylamide gels (Invitrogen, Carlsbad, CA, USA) at 200 V for 40 min, before being stained using Coomassie Brilliant Blue.

2.9. Detection of dityrosine cross-links

α–SN samples (22 μM protein/well) were subjected to SDS–PAGE as described above and then electroblotted to nitrocellulose membranes (iBlot2, Thermofisher, 25 V, 6 min). The membranes were then washed with Tris-buffered saline (TBS) and blocked with Tris-buffered saline with 0.1% Tween mixed with bovine serum albumin (TBST–BSA) for 1 h at 22 °C. The membranes were then probed with a primary mouse anti–dityrosine monoclonal antibody (Japan Institute for the Control of Aging; JaICA, 1:500 diluted in 1% BSA/TBST) overnight at 4 °C. Subsequently, the blots were washed four times with TBST for 15 min, then incubated with an anti-mouse–HRP conjugate (1:2500 in 1% BSA/TBST) for 1 h at 22 °C, and then washed four times with TBST, followed by four times with TBS at 22 °C. Bands were detected by chemiluminescence using ECL plus solution (Thermo Fisher) monitored using a SyngeneG: Box, with an automatic shutter speed.

Intrinsic fluorescence from Tyr and dityrosine was recorded at 305 nm and 405 nm respectively after excitation at 280 nm [26], using a Molecular Devices SpectraMax M2 instrument (Sunnyvale, CA, USA).

2.10. Electrospray ionization mass spectrometry (ESI–MS) analysis of α–SN samples

ESI–MS analysis of samples was performed in the positive ion mode with a SolariX XR Bruker mass spectrometer coupled to a Dionex Ultimate 3000 high–performance liquid chromatography system without a column. Samples (10 µL) were diluted with 100 µL MeOH containing 0.1% formic acid, and 100 µL deionized H_2O containing 0.1% formic acid. Samples were injected using the HyStar_LC at a flow rate of 3 µL min^{-1}. MS was operated at drying gas temperature of 200 ºC source temperature, and a capillary voltage of 4000 V. In source collision energy was 60 V whereas collision gas flow rate was 30%. The lower and upper excitation event limits were 150 and 4000 *m/z* respectively. Listed *m/z* values in the tables are given for the monoisotopic mass. Data acquisitions and analysis were carried out using Compass ftms control and Compass data analysis software, respectively.

2.11. Statistical analysis

Data are presented as the mean and standard deviations of three replicates from three independent experiments unless otherwise stated. Statistical analysis was undertaken using the packages available in Excel with $p < 0.05$ taken as significant.

3. Results

3.1. *Cu^{2+}–catalyzed modification of α–SN determined by capillary electrophoresis (CE)*

α–SN was subjected to six different sets of modification conditions at 37 °C, as indicated in the Materials and methods and Table 1, with varying molar ratios of Cu^{2+} and H_2O_2 relative to α–SN, and for varying reaction times, before analysis by CE. Analysis of the samples from the earliest time point that could be examined (0.1 min; Fig. 1A) showed a single sharp and symmetric peak that eluted at 21 min, with a 10% loss of intensity compared to native α–SN (Fig. 1A). With longer incubation times (e.g. 5 min) a significant loss of peak intensity (~75%) was observed, together with a new peak that eluted at 18 – 19 min (Fig. 1A), implying rapid modification of α–SN. At longer time points (e.g. 60 min, Fig. 1A; 360 min, Fig. 1A) almost complete loss of the native α–SN peak was observed. The broadening of the protein peaks with increasing reaction time is assigned to the presence of a heterogeneous mixture of modified α–SN species. These changes were not detected in any control sample (Supplementary texts and Fig. S1). With higher concentrations of Cu^{2+} and H_2O_2, an increased extent and rate of α–SN degradation was observed (Supplementary Fig. S2 A-C).

3.2. Quantification of protein carbonyls on modified α–SN

The carbonyl levels detected for control samples without added Cu^{2+} (Fig. S3A, Table S3) ranged from 0.0013 to 0.045 moles carbonyl per mole protein. Incubation of α–SN with Cu^{2+} alone gave higher levels (0.047 moles/mole). With the complete reaction systems containing a 1:2.3:7.8 molar ratio of α–SN (57.6 μM) : Cu^{2+} : H_2O_2 a higher level of carbonylation was detected, with the maximum yield of carbonyls of 0.092 moles/mole reached within 15 to 30 min

(Fig. 2A); this level was then maintained for several hours (Fig. S3B and Table S4). With a higher concentration of Cu^{2+} (condition 2), a significant increase in total carbonyl content (to 0.147 moles/mole; Fig. 2A and Table S4) was detected, though the time course of formation was similar to condition 1 (Fig. S3B). Compared to condition 1, higher ratios of H_2O_2 (condition 3) increased the yield of carbonyls at all time points (Fig. 2A, S3B and Table S4). With the highest concentrations of both Cu^{2+} and H_2O_2, (condition 4; Fig. 2A and Table S4) the highest yield of carbonyls was observed (0.221 moles/mole after 15 min). The time–dependence of carbonyl formation with this system was similar to conditions 1 to 3 (Fig. S3B). Spiking experiment where additional Cu^{2+} (135 μM), H_2O_2 (450 μM), and $AscH^-$ (450 μM) were individually added into the reaction mixture after 30 min did not show any significant change in the overall extent of carbonyl formation (Fig. S3D).

3.3. Effect of Cu^{2+}–catalyzed oxidation on α–SN amino acid composition

Cu^{2+}–mediated oxidative modification was examined further by amino acid analysis. The experimentally–determined amino acid composition of the 15 residues investigated for the native α–SN was very similar to the values predicted by the gene sequence (Fig. S4 and Table S5). Analysis of the control samples indicated that, except for the system containing α–SN and H_2O_2 alone, no significant decrease in any amino acid, or increase in Met sulfoxide, occurred (Fig. S5, Table S6). With α–SN, and H_2O_2 alone, a small decrease in Met was detected. This is possibly due to slow direct reaction of H_2O_2 with the thioether function of Met residues, as observed in other systems [49].

For the complete reaction system, with the lowest molar ratios of Cu^{2+} and H_2O_2 (condition 1), a rapid and significant decrease in Met content (~50% loss) was detected at the first

time point examined (0.1 min; Fig. 3A). At 5 min, 75% of the Met were modified, and a further slow decline was observed between 5 and 360 min (Fig. 3A). With an increased molar ratio of Cu^{2+} (condition 2), the loss of Met was ~40% at 0.1 min, ~80% at 5 min (Fig. S6A) and almost complete loss was detected at 360 min. Higher concentrations of H_2O_2 (condition 3; Fig. S7A) resulted in a comparatively slower modification of Met compared to higher Cu^{2+} concentrations. However, with higher levels of both Cu^{2+} and H_2O_2 (condition 4), there was an additive loss of Met (Fig. S8A). Control samples incubated for up to 360 min with EDTA alone revealed no significant loss of Met over 360 min (Fig. S5 and Table S6).

With mild oxidative conditions (condition 1) approximately 50% loss of Tyr residues was observed at the 5 min time point (Fig. 3B, Table S7), and this increased to nearly 70% by 15 min (Fig. 3B, Table S7). However, at longer time points (e.g. 60 min) the rate of Tyr loss decreased (Fig. 3B, Table S7). With higher Cu^{2+} concentrations (condition 2) a greater loss of Tyr (77%) was detected by 5 min (Fig. S6B, Table S8), and a similar increase in Tyr loss (~70%) was seen with increased H_2O_2 concentrations (condition 3) (Fig. S7B and Table S9). With higher concentrations of both reagents (condition 4) ~90% of the Tyr was consumed within 5 min, and almost complete loss was detected at longer time points (Fig. S8B and Table S10). Control samples incubated for 0 and 360 min with EDTA revealed (Fig. S5 and table S6) no Tyr loss over this time period.

With regard to His loss, mild oxidative conditions (condition 1), resulted in a significant (62%) loss after 360 min (Fig. 3B, Table S7), but with higher Cu^{2+} concentrations (condition 2), a slow accumulative loss of His was detected up to 60 min (Fig. S6B and Table S8). With higher H_2O_2 concentrations, or higher levels of both reagents (conditions 3 and 4) (Fig. S7B and S8B, Tables S9, S10), no consistent trend was detected with regard to His loss, indicating a complex molecular interplay.

3.4. Circular dichroism (CD) analysis of oxidation–induced changes in α–SN secondary structure

Figure S9 shows CD spectra of control and oxidized samples under the various oxidative conditions examined, as a function of time. All the spectra show intense negative peaks at around 195 nm typical of random coil conformations, in agreement with previous observations [50]. Mild oxidative conditions (condition 1) did not induce significant alternations (Fig. S9B), but an increase in the intensity of the negative shoulder at ~218 nm, and a decrease in the intensity of the negative band at ~198 nm, was observed for conditions 2 to 6 over time (Figs. S9C – S9G); possibly indicating a transformation from random coil conformation to a more β–rich backbone structure.

3.5. SDS analysis of oxidatively modified α–SN

Analysis of control samples (Fig. 4A) indicated the presence of monomeric α–SN as single band at ~14.5 kDa, as expected, together with low levels of a species assigned to an α–SN dimer at ~30 kDa. For the oxidized samples, the initial time point (0.1 min) showed an identical dimeric band to the controls, but with increasing reaction time under mild oxidative conditions (condition 1) increasing concentrations of bands assigned to the dimer and trimer were observed (Fig. 4B), together with a band with an apparent mass slightly smaller than the parent α–SN were detected. The latter band is assigned to either a truncation or an altered conformation of the α–SN. At longer time points (15 – 360 min) under the same conditions, more pronounced formation of SDS– and heat–stable dimer, trimer, and tetramer were detected (Fig. 4B), together with a loss

of the parent α–SN band (Fig. 4B). Higher levels of Cu^{2+} (condition 2; Fig. S10A) accelerated the formation of dimer, trimer, and tetramer and loss of parent protein band (Fig. S10A). Higher H_2O_2 concentrations (condition 3) showed less prominent dimer, trimer, and tetramer bands over time, and more diffuse (smeared) bands were observed after 360 min of incubation (Fig. S10B). Higher levels of both Cu^{2+} and H_2O_2 (condition 4) gave less intense bands for all species (Fig. S10C) consistent with an overall loss of total native protein.

3.6. Detection of dityrosine cross-links

To probe whether the dimer, trimer, and tetramer seen by SDS–PAGE and pre-fibrillar oligomers (molecular weight higher than a tetramer of α–SN) arise via dityrosine cross-linking, Western blotting was conducted using an anti–dityrosine antibody. No dityrosine was detected for control samples except for α–SN incubated with Cu^{2+} alone for 360 min at 37 ºC, which showed weak staining (Fig. 5A). However, α–SN samples subjected to the complete oxidation system (condition 1) showed a time-dependent increase in dityrosine–positive bands (Fig. 5A, lanes 5 – 10), with little dityrosine detected at the earliest time point (0.1 min), but significant formation at later times, with staining of the monomer, dimer, trimer, tetramer, and pre-fibrillar oligomer bands. With increasing incubation time, the dityrosine staining was detected primarily at the molecular mass of the pre-fibrillar oligomeric species (Fig. 5A). These data were corroborated by intrinsic fluorescence measurements, where a rapid loss of the intrinsic Tyr fluorescence signal (305 – 310 nm) with an accompanying increase in fluorescence emission intensity at 405 – 410 nm, was detected with increasing incubation time with the complete oxidation system (Fig. S11A). Control samples showed no change in Tyr or dityrosine fluorescence intensity. With higher Cu^{2+} concentrations, a similar trend to that seen with

296 condition 1 was detected, however, the extent of formation was faster and more defined (Fig. 5B,
297 lanes 1 to 5).
298
299 ***3.7. ESI–MS analysis of modified α–SN***

300 ESI–MS analysis of control α–SN revealed an extended population with charge state ions
301 of 11+ to 19+ (Fig. S12). As the 14+ charge state gave rise to the most intense peaks, further
302 analyses concentrated on this state (Fig. S12A). Within the extended 14+ series, the MS spectrum
303 showed species with $[\alpha\text{–SN} + H]^+$, $[\alpha\text{–SN} + H + 18]^+$, and $[\alpha\text{–SN} + H + 58]^+$ corresponding to
304 monoisotopic *m/z* values of 1033.25, 1034.54, and 1037.39, respectively (Fig. 6, Fig. S12B,
305 Table S13). The + 18 Da (1O + 2H) and + 58 Da products (acetylated α–SN + 1O) were of much
306 lower abundance than the protonated α–SN ion ($[\alpha\text{–SN} + H]^+$) (Fig. S12B, Table S13). The
307 simulated MS spectra for the unoxidized–α–SN, α–SN + 18 Da, and α–SN + 58 Da α–SN species
308 (Figs. S12C – S12D), showed an identical monoisotopic *m/z* distribution. This suggests only
309 minimal α–SN modification during purification and handling.

310 ESI–MS analysis of α–SN exposed to condition 1 for varying time periods is shown in
311 Fig. 6 and Table S14. The 0.1 min sample gave rise to a mixture of signals, the most prominent
312 of which had mono isotopic *m/z* values of 1034.39 (+ 16 Da), 1035.54 (+ 32 Da), and 1036.68 (+
313 48 Da) corresponding to three distinct oxidized and protonated α–SN species. The 5 min sample
314 (Fig. 6C, Table S14) showed complete loss of the *m/z* 1033.25 signal corresponding to
315 unmodified α–SN, and new species with *m/z* values of 1036.46 (+ 45 Da; + 3O – 3H), 1035.32 (+
316 30 Da; + 2O – 3H), 1037.60 (+ 62 Da; + 4O – 3H) and 1034.18 (+ 13 Da; + 1O – 3H). These
317 values corresponding to the addition of three, two, four and one oxygen (O) atoms and the loss of
318 3 hydrogen (–3H) atoms from each species (Table S14). The 15 min sample gave intense ions

with *m/z* 1037.46 and 1036.39, corresponding to (+ 59 Da; + 4O – 3H) and (+ 44 Da; + 3O – 3H) suggesting incorporation of four and three oxygen atoms, respectively (Fig. 6D, Table S14). The abundance of acetylated α–SN present in the control samples decreased, and the abundance of this species with oxidative modifications increased, with increasing incubation time between 0.1 – 15 min (Table S14).

3.8. Effect of ascorbate ($AscH^-$) on Cu^{2+}–catalyzed damage to α–SN

The addition of $AscH^-$ to the mild oxidative reaction conditions (i.e. condition 1 with $AscH^-$ at the same molar ratio as H_2O_2; condition 5, Table 1) resulted in more rapid changes to the species detected with CE (Fig. 1B). Thus the 0.1 min time point sample showed a 50% loss of intensity compared to the unoxidized sample and the appearance of two new peaks at 18 (weak) and 21 min. At longer time points the parent α–SN peak continued to decrease in intensity, whilst the peak at 21 min increased, then remained at a plateau value for the remaining time period examined (Fig. 1B). With higher concentrations of $AscH^-$ (condition 6; Table 1, Fig. S2D), the overall migration pattern of oxidized α–SN remained the same. Control samples showed no significant changes (Fig. S1).

The presence of $AscH^-$ (as above) also modulated the yield and time course of protein carbonyl formation, with a rapid initial increase, and then a plateau level of carbonyls detected over the remaining incubation time (Fig. 2B). This plateau level was not significantly different with the two different $AscH^-$ concentrations. The initial rate of increase in the presence of $AscH^-$ was more rapid than seen in the absence of $AscH^-$, but the plateau level was much lower (~0.07 moles/mole; Fig. 2B, Table S4), than for all of the conditions (1 – 4) in which $AscH^-$ was not present (Fig. 2A).

Consistent with the above time course data, analysis of the consumption of parent amino acids, and formation of Met sulfoxide, in the presence of $AscH^-$ showed significant differences to the absence of $AscH^-$. After 0.1 min incubation with mild oxidative conditions with $AscH^-$ present (condition 5), ~50% of the Met residues had been converted to Met sulfoxide (Fig. 3C), and these values remained constant at longer incubation times. With the higher concentration of $AscH^-$, and the highest concentrations of Cu^{2+} and H_2O_2 (condition 6), ~ 3 Met residues were lost by the 0.1 min time point, and this remained constant at longer time points (Fig. S13A). For Tyr residues, a similar rapid, but lower overall loss was detected compared to the absence of $AscH^-$. Thus ~ 33% Tyr was lost at 0.1 min, and by 360 min incubation only ~ 38% was consumed (Fig. 3D and Table S11), and these levels were not significantly greater with the higher molar ratios of Cu^{2+}, H_2O_2, and $AscH^-$ (Fig. S13B and Table S12). In contrast to the above, a more significant decrease in the levels of His were detected in the presence of $AscH^-$ compared to its absence (Fig. 3D, Table S11 with ~42% His oxidized after 0.1 min, and a further slow loss detected at 15 min (~65%), after which the values remained unchanged (Fig. 3D, Table S11). A similar trend was seen for the incubations with higher molar ratios (condition 6; Fig. S13B, Table S12).

Consistent with the above data, less dramatic changes were seen for the α–SN samples examined by SDS–PAGE in the presence compared to absence of $AscH^-$ (Fig. 4C, Fig. S10D). Formation of the dimer, trimer, tetramer, and pre-fibrillar oligomer bands were not detected above those detected for controls. The presence of $AscH^-$ also decreased the intensity of the band detected at slightly lower mass than the parent α–SN (Fig. 4C vs. 4B), though an additional low-intensity band was detected at ~ 4.5 kDa for both conditions 5 and 6 (Figs. 4C, and S10D), which was not detected in the absence of $AscH^-$. Consistent with the minor consumption of Tyr detected by amino acid analysis, only low-intensity dityrosine bands resembling monomer were

365 detected by Western blotting (Fig. 5B, lanes 6 – 10). This observation is further supported by
366 limited loss of the intrinsic fluorescence of Tyr at 305 – 310 nm (Fig. S11B), or insignificant
367 increase in dityrosine at 405 – 410 nm (Fig. S11B inset).

368 Consistent with the rapid rate of Met and Tyr loss and protein carbonyl formation
369 detected in the presence of $AscH^-$, ESI–MS analysis of the samples oxidized in the presence of
370 $AscH^-$ showed extensive modification at the 0.1 min time point (Fig. 7, Table S15), with an
371 intense signal with monoisotopic *m/z* values of 1036.6 (+ 47 Da) detected. This species was the
372 most prominent ion detected for the 0.1 min, 5 min, and 15 min time points, and corresponds to
373 the addition of three oxygen atoms to a protonated α–SN and loss of a hydrogen atom. Oxidized
374 α–SN species with 1 to 6 added oxygen atoms on protonated α–SN were also evident at the 0.1
375 min time point, with only low levels of ions from unmodified α–SN (*m/z* 1033.25). This ion was
376 not however detected at the 5 and 15 min time points (Fig. 7C, D, and Table S15) consistent with
377 complete loss of parent α–SN (cf. the CE data). Acetylated α–SN was also detected with
378 oxidative modifications.

379

380 ## 4. Discussion

381 ### *4.1. The mechanism of metal-catalyzed protein oxidation*

382 Our understanding of the factors and particularly the role of oxidatively generated damage
383 that contribute to early α–SN aggregation/oligomerization is limited. Oxidatively generated
384 damage to α–SN by metal ion– and/or H_2O_2–mediated systems has not been completely
385 elucidated, and the available data are somewhat contradictory due to the harsh oxidative
386 conditions used in some studies (Table S1) [20, 24, 26, 31, 39-41]. The high Cu^{2+} / H_2O_2

concentrations and molar ratios to α–SN employed, and the use of chelating buffers makes extrapolation from these studies to *in vivo* studies difficult. Intracellular local concentrations of α–SN are suggested to be ~20-100 μM in the brain where α–SN is naturally abundant [51]. The intracellular copper ion concentrations has been reported to reach up to 15 μM in brain synaptosomes and ~300 μM in synaptic vesicles where α–SN is enriched [52]. Additionally, evidence has been also put forward for a dynamic pool of loosely bound copper ions that could interact with α–SN [53]. The current study was designed to use concentration not too far from these biological conditions.

Of the previously examined metal ion–catalyzed systems [54], the Cu^{2+}/H_2O_2 system was chosen, as elevated Cu^{2+} concentrations have been linked to elevated oxidative stress [35], oligomerization of α–SN [32] and Lewy body formation [26]. The mechanism for the reaction in the absence of $AscH^-$ has been suggested to be [55]:

(I) $Cu^{2+} + H_2O_2 \rightarrow Cu^{+} + O_2^{-\bullet} + 2\ H^{+}$

(II) $Cu^{2+} + O_2^{-\bullet} \rightarrow Cu^{+} + O_2$

(III) $Cu^{+} + H_2O_2 \rightarrow Cu^{2+} + HO^{-} + HO^{\bullet}$

In the presence of $AscH^-$, the reduction of Cu^{2+} by $AscH^-$ could facilitate production of Cu^+ as described by the equation below [56].

(IV) $Cu^{2+} + AscH^{-} \rightarrow Cu^{+} + Asc^{-\bullet} + H^{+}$

Although extensively studied, the oxidizing species produced by reaction of protein-copper complexes with H_2O_2 remains contentious. Several studies focused on DNA damage mediated by Cu^{2+} and H_2O_2 suggests that HO· is not the main radical species [57]. It has been assumed that

the reduction of protein-bound Cu^{2+} to Cu^{+}, can take place by either H_2O_2 (reaction I) or by superoxide radical anions. Cu^{+} can then participate in a Fenton-like reaction with additional H_2O_2 (reaction III). This would generate Cu^{2+}-$HO^{\bullet}$ or its ionized equivalent, Cu^{2+}-$O^{-\bullet}$, as proposed earlier [58]. Although not examined here in detail, we do not rule out the possibility that more than one active species is involved in random and site-specific damage to α-SN.

The effect of multiple different molar ratios of Cu^{2+}/ H_2O_2/ $AscH^{-}$ were evaluated over time up to 360 min (Table 1), with the experiments carried out using 20 mM MOPS–NaOH, pH 7.4, as this buffer does not complex Cu^{2+} readily, is stable and is not readily oxidized under the conditions employed [59].

4.2. Side-chain carbonylation is not one of the major early events in MCO of α–SN

CE provides a robust platform [60] to examine the effects of Cu^{2+}, H_2O_2, and $AscH^{-}$ on α–SN. The peak from native α–SN was converted to multiple additional species over the time course examined with the rate and extent of this process depends on the presence and concentrations of Cu^{2+}, H_2O_2 and $AscH^{-}$ (Figs. 1, and S2). Protein oxidation is known to generate various chemical as well as structural modifications, including altered charge and conformation. Such oxidatively induced modifications would result in different electrophoretic migration and can be monitored by CE as shown previously [61]. Figure 1A shows electrophoretic migration of control and oxidized α-SN under condition 1. Two small peaks with migration time ~18 - 19 min can be seen at the earliest time interval (0.1 min), with increasing intensity of same peaks up to 60 min. The rapid formation of Met sulfoxide and dityrosine as observed by amino acid and western blot analyses within the same time interval (0.1 – 60 min) suggests that these newly formed peaks with changed electrophoretic migration may represent isoforms with Met and Tyr oxidations. It is interesting to note that the near disappearance of native α-SN peak correlates

with the loss of native α-SN band on SDS-PAGE (Fig. 4B). The loss of peak resolution after 60 min could be due to the heterogeneous mixture of oxidized α-SN species as judged by western blot (Fig. 5B). On the other hand, the near absence of the peaks in figure 1B under condition 5 (condition 1 with $AscH^-$) appears to reflect limited Met and Tyr oxidation. These data, and also those from the other complementary techniques employed, indicate that major changes to α–SN occur over a period of seconds to minutes and that the rate of change is considerably slower after 15 min. The presence of $AscH^-$ (conditions 5 and 6) markedly changed the observed behavior, with this occurring more rapidly, but also to a lower overall extent, with a rapid "burst" of oxidation on the seconds time scale, followed by near plateau values over the remaining time period. Furthermore, the different pattern of peaks detected by CE, the changes in protein carbonyl levels, the differences in amino acid consumption, and the bands detected by SDS–PAGE, are consistent with different processes occurring in the presence of $AscH^-$.

Although protein-bound carbonyls are widely used as a biomarker, and a quantitative measure of oxidative stress [5, 62], previous studies on α–SN [24, 38, 39] have not measured carbonyl formation. The data obtained here show, with a wide variety of different concentrations and molar ratios of Cu^{2+}, H_2O_2, and $AscH^-$ that: i) limited carbonyl formation occurs within the first 5 min of reaction with Cu^{2+}/ H_2O_2 system; ii) that the Cu^{2+} concentration is a major driver of the extent of this process; iii) that α–SN can be oxidized in the absence of reducing agents; and iv) that carbonyl generation follows a similar time course under all of the conditions examined (Figs. 2 and S3). However, the overall levels of protein carbonyls detected all of the conditions examined is rather low and reaches a maximum level of only ~20% of the α–SN molecules carrying a single carbonyl function. The plateau values detected for the carbonyl levels could be due to depletion of H_2O_2 or Cu^{2+} in the solution. Thus, whenever Cu^+ is formed some fraction will disproportionate according to the equation:

(V) $2\ Cu^{+}(aq) \leftrightarrows Cu$ and $Cu^{2+}(aq)$

This would be expected to slowly remove Cu^{2+} ions from solution as metallic copper thereby slowing down the observed rate of oxidation. However, the spiking experiments where more Cu^{2+}, H_2O_2, and $AscH^-$ were individually added to the reactions after 30 min suggest that this is not the complete reason for the plateau values and that other factors must play a significant role.

The stimulation of protein carbonyl formation in the presence of $AscH^-$ compared to its absence (i.e. condition 5 vs. condition 1), may arise from enhanced reuduction of Cu^{2+} to Cu^{+} (reaction IV) by $AscH^-$. The higher concentration of Cu^{+} might increase the initial rate of carbonyl formation (reaction III), allowing a rapid initial burst of carbonyl generation at early stage of MCO. However, due to potential radical scavenging ability of $AscH^-$, the overall carbonyl generation could be lowered by means of i) limiting the concentration of reactive species that react with the α–SN (i.e. via direct scavenging of the initial oxidant species [63]; and ii) by repair of initial radical species formed on the α–SN, a rapid process demonstrated for Tyr phenoxyl radicals [64]. Despite the different time courses of carbonyl formation detected with the Cu^{2+}/H_2O_2 and the $Cu^{2+}/H_2O_2/AscH^-$ systems, the carbonyl content in both systems rapidly reached a plateau value after 30 – 60 minutes (Fig. 2). Similar observations on the extent of overall carbonyl production have also been reported for bovine serum albumin (BSA) [65] and β-lactoglobulin [66] when subjected to Cu^{2+}/ H_2O_2 oxidation. It has been suggested that carbonyl compounds are not the final product in the oxidation reaction and that they can be converted into carboxylic acid either by auto-oxidation or by reaction with H_2O_2 [67]. Furthermore, lysine residues can diminish the carbonyl content, by forming either Schiff base compounds or other

cross-links [66]. If so, the relatively large number of lysine residues (15) present in α–SN may help account for the absence of further increases in carbonyl production. It is also noting that most rapidly and readily oxidized residues such methionines and tyrosines as in case of α–SN do not give high yields of carbonyls as products. Thus, although carbonyl levels are often used as an indicator of protein damage [68], our data indicate that significant damage to α–SN may occur prior to a significant increase in the overall protein carbonyl level.

4.3. Methionine oxidation occurs rapidly during MCO of α–SN

The amino acid analysis of α–SN carried out at different time points, and with different concentration of Cu^{2+}, H_2O_2, and $AscH^-$, confirms the rapid time course of changes in the protein and the occurrence of different reaction pathways. In the absence of added Cu^{2+}, but with added H_2O_2, a slow loss of ~1 Met and formation of 1 mole of Met sulfoxide was detected, consistent with slow molecular oxidation at a single reactive Met residue (Fig. S5 and Table S6). All other control samples showed no measurable changes (Fig. S5 and Table S11). In the presence of the complete oxidation system (but without $AscH^-$) rapid oxidation of two (on average) of the four Met residues in α–SN (Met–1, Met–5, Met–116, and Met–127) was detected by the 0.1 min time point. The other two Met residues were consumed more slowly, but oxidation of all the Met residues was essentially complete by 360 min (Figs. 3A, S6A, S7A, and S8A). This stepwise Met oxidation can be rationalized by the presence of a high–affinity Cu^{2+} binding site [32, 69] located in the N–terminal region of α–SN where Met–1 and Met–5 are located. The formation of oxidants from H_2O_2 by Cu^{2+} bound at this site could result in rapid oxidation of these two N–terminal Met residues followed by slower oxidation of the C–terminal Met–116 and Met–127 [70]. This observation is supported by ESI MS analyses (*vide infra*). However, it is interesting to note that whilst the mildest oxidation system (condition 1) showed immediate Met oxidation to Met

sulfoxide (Fig. 3A), increasing the molar ratio of Cu^{2+} (condition 2; Fig. S6A), and an increased molar ratio of H_2O_2 (condition 3; Fig. S7A), as well as increase molar ratio of both Cu^{2+}/ H_2O_2 (condition 4; Fig. S8A), appeared to slow down the rate of conversion of Met to Met sulfoxide, possibly due to Cu^{2+} coordination with either α–SN [71], or products of the initial reaction (e.g. a sulfoxide–α–SN species). Inter– as well as intra–molecular coordination of multiple Met sulfoxides with metal ions, have been suggested to alter fibrillation process of α–SN [31, 34]. Indeed, the more rigid and polar Met sulfoxide may alter protein structures [72] and result in conformational transitions of the protein [73]. Thus, lower Cu^{2+} concentrations may favor a more rapid oxidation of Met residues. Met sulfoxide has also been suggested to disrupt end–to–end association of α–SN and thus be inhibitory to fibrillation of α–SN [74]. In line with this data, Cu^{2+} has been reported to accelerate α–SN aggregation with an inverse relationship to the Cu^{2+} concentration; however, the aggregation growth (k_{app}) is not affected by overall Cu^{2+} ion concentration [32].

$AscH^-$ is known to exhibit "crossover" effect as pro vs. antioxidant [75] depending on its concentrations [76].When $AscH^-$ was added to the mild oxidation system (condition 1) to give condition 5, only two Met residues were oxidized over the 360 min (Fig. 3C). Interestingly, a recent study has reported an intracellular repair mechanism where oxidized N–terminal Met residues (Met–5 and Met–1) are repaired in a stepwise manner. However, the two C–terminal species (Met–116 and Met–127) were oxidized to Met sulfoxide [70]. Thus the presence of $AscH^-$ may modulate the overall oxidation process by a continuous recycling of the N–terminal Met residues. However, an additive effect of Cu^{2+} and H_2O_2, with $AscH^-$ was seen in condition 6 (Fig. S13A), where three of four Met residues were fully oxidized by 360 min. Furthermore, the concentration of Met sulfoxide does not appear constant with this decreasing after 5 min

incubation (Fig. S13A), consistent with further reaction, possibly to the sulfone. This observation is in agreement with the detection of Met sulfone under strongly oxidizing conditions [77].

4.4. Intra- and inter-molecular dityrosine formation is one of the major early events in MCO of α–SN

It is established that the formation of dityrosine cross-links involves the transient generation of Tyr-derived phenoxyl radicals by one-electron oxidants [78], whereas Met sulfoxide can be generated by both two- and one-electron oxidation reactions [79]. The four Tyr residues at positions 39, 125, 133, and 136 have been implicated in the pathogenesis of PD via dityrosine covalent cross-linking [26]. However, previous studies have not demonstrated early conversion of these residues to dityrosine crosslinks. The amino acid analysis reported here indicate that Tyr loss is an early event, with two Tyr residues consumed after 5 min incubation (Fig. 3B), and ~3 three Tyr lost after 360 min. The rapid loss of Tyr under conditions 1 – 4, suggests that the Cu^{2+} ion concentration is a major molecular driver of damage via Tyr–Tyr coupling. However, inhibition of dityrosine formation in the presence of $AscH^-$ may occur via removal of tyrosyl radicals.

4.5. Site-specific oxidation of His–50 in the presence of $AscH^-$

Oxidation of the His residue in α–SN with low Cu^{2+} concentrations (condition 1) appears to be slower than for some of the Met and Tyr residues. This may be due to a binding interaction of His–50 with Cu^{2+}. The imidazole ring of His–50 is one of the Cu^{2+} binding sites at the N-terminus of α-SN [80]. An explanation for the oxidation of His–50 in the presence of $AscH^-$ (condition 5) could be that, His–50-bound Cu^{2+} can be reduced to Cu^+, which then interacts with

exogenous H_2O_2 to oxidize the H50 side chain in a site-specific manner through copper coordination (Fig. 3D). Another possibility is that, in the presence of $AscH^-$ the Fenton-like reaction of Cu^+ with H_2O_2 would specifically generate diffusible $HO^\bullet$, which then reacts at diffusion control with nearby residues such as His–50. The redox cycling of His–50–bound Cu^{2+}, as well as a site-specific oxidation of His–50 in the presence of $AscH^-$, shown in this study, supports the role of His–50 residues in copper coordination [81].

4.6. Copper-ion catalyzed oxidation and structural changes in the absence and presence of $AscH^-$

The CD spectra obtained (Fig. S8) show random coil conformations for all the α–SN samples examined, with only modest, and poorly informative, differences between the conditions. More informative data was obtained by SDS–PAGE. Oxidation in the absence of $AscH^-$ resulted in dimer, trimer, tetramer, and pre-fibrillar oligomer formation, with the extent dependent on the oxidant concentrations (Fig. 4). These bands were shown to contain dityrosine by Western blotting (Fig. 5). Incubation for 5 min, in the absence of $AscH^-$, was sufficient to show a marked increase in (non–reducible and heat–stable) dityrosine formation, with the majority of the staining progressively appearing higher up the gel (i.e. at higher average molecular masses) with longer incubation times (Fig. S11A), consistent with rapid formation of dityrosine and pre-fibrillar oligomer assembly. The gradual decrease in overall dityrosine signal intensity (Fig. S11C) is possibly due to inaccessibility of the antibody to the antigen in the highly aggregated material.

In contrast, when $AscH^-$ was present, no formation of dimer, trimer, tetramer, and pre-fibrillar oligomer bands were detected by either SDS–PAGE gel (Fig. 4C), and Western blotting (Fig. 5B) or direct fluorescence measurements (Fig. S11B and S11C). This is consistent with

574 rapid repair of Tyr phenoxyl radicals by $AscH^-$ [82, 83], and suggests a key role for $AscH^-$ in
575 limiting modification of α–SN.

576 The ESI–MS analysis confirmed the rapid oxidation α–SN in both the absence and
577 presence of $AscH^-$. The data obtained are consistent with limited and very rapid modification of
578 Met residues within the first fraction of a minute. Subsequent formation of dityrosine cross-links
579 in the absence of $AscH^-$ as indicated by the loss of one to three or two H atoms (1–3 Da),
580 indicative of both inter– or intramolecular cross-links (Table S14). Also in the absence of $AscH^-$,
581 the Western blotting data suggest that inter–molecular linkages are more prevalent, with most of
582 the staining detected in oligomer bands. However, in the presence of $AscH^-$, only very low-
583 intensity dityrosine bands as detected by Western blotting (Fig. 5B, lanes 6 – 10). The amino acid
584 analysis (Fig. 3) also suggest that Met sulfoxide may not be the final product arising from
585 oxidation of this residue in the presence of $AscH^-$, though with only slow conversion of Met
586 sulfoxide (+16 Da) to sulfone (+32 Da). The MS results from the 0.1, 5 and 15 min samples in
587 the presence of $AscH^-$ (Fig. 7, Table S15) indicate that there are 1 – 6 oxygen species attached to
588 protonated α–SN. Even at 0.1 minute oxidation the highest intensity is the peak with *m/z* values
589 of 1036.6 (+ 47 Da; + 3O – 1H), consistent with very rapid conversion of Met residues to Met
590 sulfoxide.

591 ***4.7. Physiological relevance of copper-ion catalyzed oxidation of α–SN in the absence and***
592 ***presence of $AscH^-$***
593
594 The pathogenesis of Parkinson's disease includes compromised cell membrane integrity,
595 mitochondrial stress, synaptic dysfunction, and general cellular toxicity [84]. However, the
596 primary pathogenic agents in these conditions are thought to be the prefibrillar species that are

intermediates during the self-assembly of α-SN, and toxic effects of such prefibrillar been have reported [85].

Collectively, our studies shows that brief exposure of α-SN to a Cu^{2+}/H_2O_2 system without $AscH^-$ leads to a rapid and complete oxidation of two crucial amino acid residues; i.e.; methionine and tyrosine (Figs. 3A and 3B), which are implicated in the toxicity of α-SN. Oxidation of methionine and tyrosine residues are known to inhibit fibrillation of α-SN and thereby formation of stable soluble α-SN oligomers [86]; which are central to PD pathogenesis [85]. In vitro and in vivo studies have shown that the oxidation of methionine in α-SN i) impairs its degradation by the 20S proteasome [87], ii) decreases its affinity for membranes [88], and iii) promotes the formation of cytotoxic α-SN oligomers [89]. Furthermore, C-terminal methionine sulfoxides are suggested to reduce the phosphorylation of Tyr125 by tyrosine kinase Fyn; which has been linked to age- and disease-dependent decline of Tyr125 phosphorylation both in a Drosophila PD model and in humans [90]. Previous work has also revealed that Lewy bodies in PD patient brain tissues contain dityrosine cross-linked α-SN oligomers [26]. Studies using animal models have suggested that the dityrosine cross-linked dimers may play an important role in oligomer toxicity [91]. Furthermore, seeding experiments with dityrosine cross-linked dimers are found to accelerate α-SN fibril growth indicating dityrosine cross-linked dimeric α-SN species to rate-limiting step in the nucleation of α -syn fibrils [92]. In line with previous observations, our data demonstrate the formation of SDS- and heat-stable dityrosine cross-linked α-SN oligomers and the oxidation of methionines within 5 min (Figs. 4 and 5). These species are potential early intermediates in the formation of toxic prefibrillar α-SN oligomers.

When α–SN was exposed to the $Cu^{2+}/H_2O_2/AscH^-$ mixture, more limited oxidation of two Met residues and one Tyr residue was detected (Fig. 3C and 3D), with a near total absence of dityrosine-containing cross-linked dimer, trimer, tetramer, and pre-fibrillar oligomer bands as

judged by SDS–PAGE and Western blot analysis (Figs. 4C and 5B). However, significant His–50 oxidation was detected under these conditions in a site-specific manner (Fig. 3D). To counteract the oxidative imbalance leading to intracellular damages to the proteins, several subcellular compartments contain sophisticated repair machinery including $AscH^-$ [93, 94]. $AscH^-$ is a strong reducing agent, which can reduce transition metal ions including Cu^{2+}. $AscH^-$ is also known to act as pro- and antioxidant depending on its concentrations [75, 93]. Remarkably, when α-SN was exposed to $Cu^{2+}/H_2O_2/$ $AscH^-$ system, oxidation of only two methionines was observed (Fig. 3C). Met–5 and Met–1 at the N-terminus constitutes the major Cu^{2+} binding site of α-SN [80]. Thus the presence of $AscH^-$ in the reaction (condition 5) may lead to the site-specific oxidation of Met–5 and Met–1. However, at any given time interval only two Met were oxidized to Met sulfoxide (Fig. 3C). $AscH^-$ is also known to efficiently repair protein-thiol and protein-Tyr radicals [95, 96]. At this point, we can only speculate that the two C–terminal Met (Met–116 and Met–127) remain fully oxidized as Met sulfoxide. This observation is further supported by a previous study where intracellular repair enzyme, methionine sulfoxide reductase (MSR) failed to repair Met–116 and Met–127 [70]. Irrespective of the $AscH^-$ concentration used in this study, the experiments showed consumption of on average about one Tyr residue (Fig. 3D, Fig. S13B). This observation indicates that i) the oxidation of Tyr residues may not involve site-specific reactions as these residues are not involved in copper coordination [97] and ii) $AscH^-$ may prevent oxidative damage to specific Tyr residues. It has been shown that Tyr phenoxyl radicals (reaction VI), a precursor of dityrosine, react rapidly with both the superoxide radical anion (reaction VII) [98, 99] and also $AscH^-$ (reaction VIII) [100]. Thus, $AscH^-$ can both accelerate the decay of Tyr phenoxyl radicals consistent with the repair of protein radicals and inhibit the formation of these species in a concentration-dependent manner [94]. These reactions are consistent with the complete disappearance of dityrosine formation in the presence of $AscH^-$ [99].

645

646 (VI) $Tyr\text{-}H + HO^{\bullet} \rightarrow Tyr^{\bullet} + H_2O$

647

648 (VII) $Tyr^{\bullet} + O_2^{-\bullet} + H^{+} \rightarrow Tyr\text{-}H + O_2$

649

650 (VIII) $TyrO^{\bullet} + AscH^{-} \rightarrow TyrOH + Asc^{-\bullet}$

651

652 In summary, this is the first systematic study providing experimental evidence of early
653 molecular events related to oxidatively -damage to α-SN. Using the Cu^{2+}/H_2O_2 oxidation system
654 we have demonstrated that both Met and Tyr oxidation precedes significant carbonyl formation
655 and the oxidation of Met and Tyr residues can be observed as early as 5 min; leading to a rapid
656 Met sulfoxide formation and dityrosine cross-linked pre-fibrillar oligomer assemblies. Such pre-
657 fibrillar species of α-SN have been suggested to exert damaging effects, via both intra- and extra-
658 cellular mechanisms [85]. In contrast, the $Cu^{2+}/H_2O_2/AscH^{-}$ oxidation system resulted in an
659 "oxidative burst" with early carbonylation and site-specific oxidation of His–50. However, the
660 dityrosine cross-linked pre-fibrillar oligomer assemblies were completely inhibited in the
661 presence of $AscH^{-}$ and only limited amounts of Met sulfoxide was formed. This indicates a
662 potential protective role of $AscH^{-}$ against oxidatively generated damage to α-SN. Our results
663 highlight the early events leading to α-SN oxidation and may advance our understanding of the
664 pathogenesis of other protein conformational diseases such as Alzheimer's and Prion disease.
665 Taken together, our data presented here using Cu^{2+}/H_2O_2 oxidation provide increasing evidence
666 that oxidative stress plays a mechanistic role in the onset/progression of PD and related
667 synucleinopathies. Although $AscH^{-}$ can show both pro- and anti-oxidant effects, the majority of
668 the literature supports an antioxidant effect *in vivo.* Anti-oxidant effects of $AscH^{-}$ could, decrease

669 Cu-mediated oxidative damage to α-SN, and may be an effective strategy against PD and related
670 disorders [93, 94]. Further studies are underway to investigate the transient formation of α-SN
671 dimers and oligomers to assess their toxicity and cell permeability.

672

673 **Acknowledgements**

674 We gratefully acknowledge financial support from the Danish Council for Independent Research
675 Technology and Production Sciences (Grant no.: DFF| FTP 4005–00082 to IMM). MJD
676 gratefully acknowledge financial support from the Novo Nordisk Foundation (Grant no.: NNF
677 13OC0004294). MKT, MJB and MJD also acknowledge financial support from the Lundbeck
678 Foundation postdoctoral fellowship to MKT (Grant no.: R231-2016-3276).

679

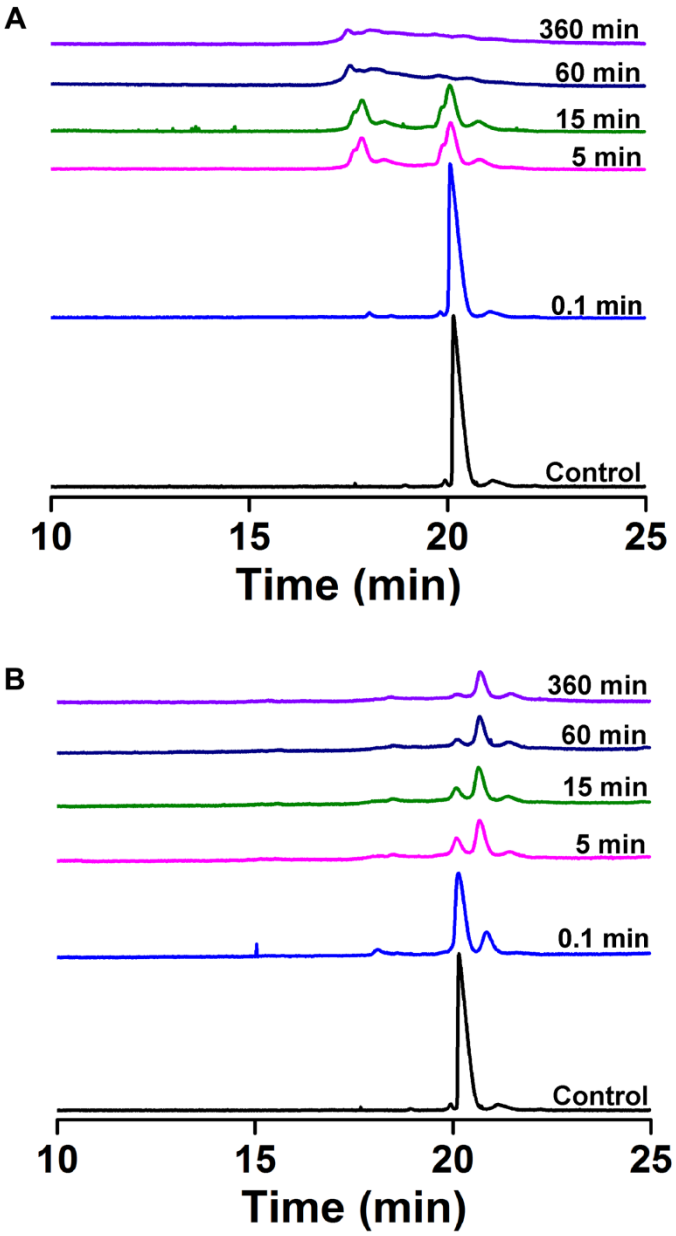

680

681 **Figure 1. Cu^{2+}/H_2O_2–mediated oxidation of α–SN in the absence and presence of ascorbate ($AscH^-$).**
682 Overlayed time-dependent capillary electrophoresis (CE) electropherograms of control and oxidized α–
683 SN. (**A**) 57.6 μM of α–SN subjected to oxidation using a Cu^{2+}/H_2O_2 system with a molar ratio of 1:2.3:7.8
684 between α–SN: Cu^{2+}: H_2O_2 (Condition 1). (**B**) 57.6 μM of α–SN subjected to Cu^{2+}/H_2O_2 / $AscH^-$ oxidation
685 using a molar ratio of 1:2.3:7.8:7.8 between α–SN: Cu^{2+}: H_2O_2: $AscH^-$ (Condition 5). Except for the 0.1
686 min sample, all other reaction mixtures were incubated at 37 °C for the time shown in the figure.

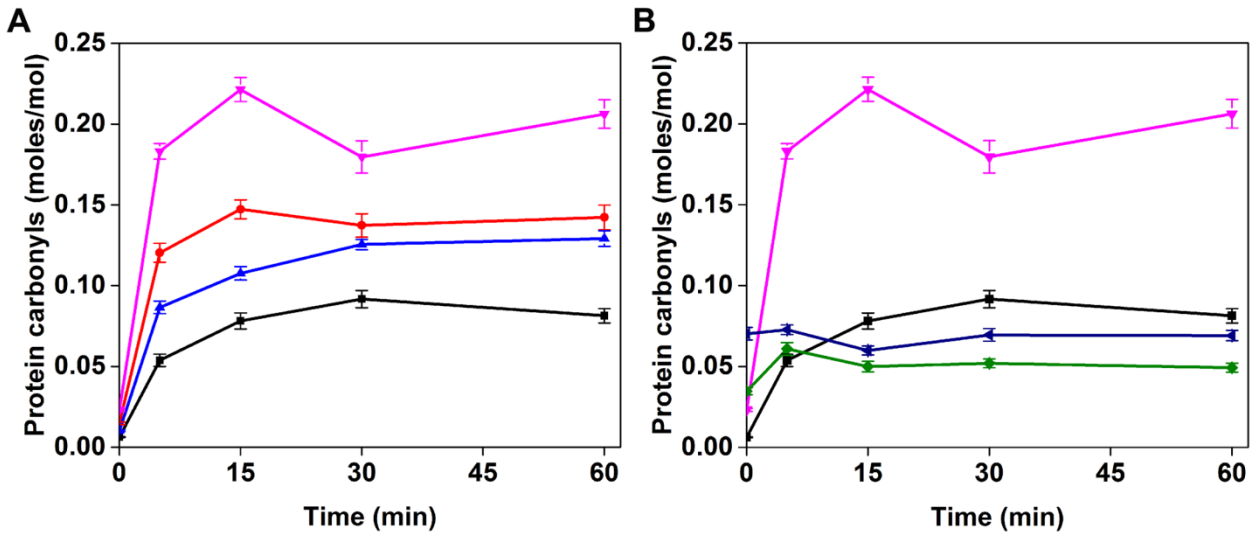

Fig. 2. Time-dependent formation of carbonyls on α–SN induced by Cu^{2+}/H_2O_2–mediated oxidation in the absence and presence of $AscH^-$. Time–course of protein carbonyl formation resulting from oxidation of α–SN (57.6 μM) in the absence and presence of $AscH^-$; (**A**) Condition 1 (black) with molar ratio of 1:2.3:7.8:0, condition 2 (red) with molar ratio of 1:4.7:7.8:0, Condition 3 (blue) with molar ratio of 1:2.3:15.6:0, Condition 4 (pink) with molar ratio of 1:4.7:15.6:0. (**B**) $Cu^{2+}/H_2O_2/AscH^-$ mediated oxidation (condition 5) (green) with molar ratios 1:2.3:7.8:7.8, and condition 6 (blue) with molar ratio of 1:4.7:15.6:15.6. Protein carbonyl levels are given as moles carbonyl/mole protein, and the data points and error bars represent the means and standard deviation of three independent experiments. Except for 0.1 min samples, all other reaction mixtures were incubated at 37 °C for the time intervals shown.

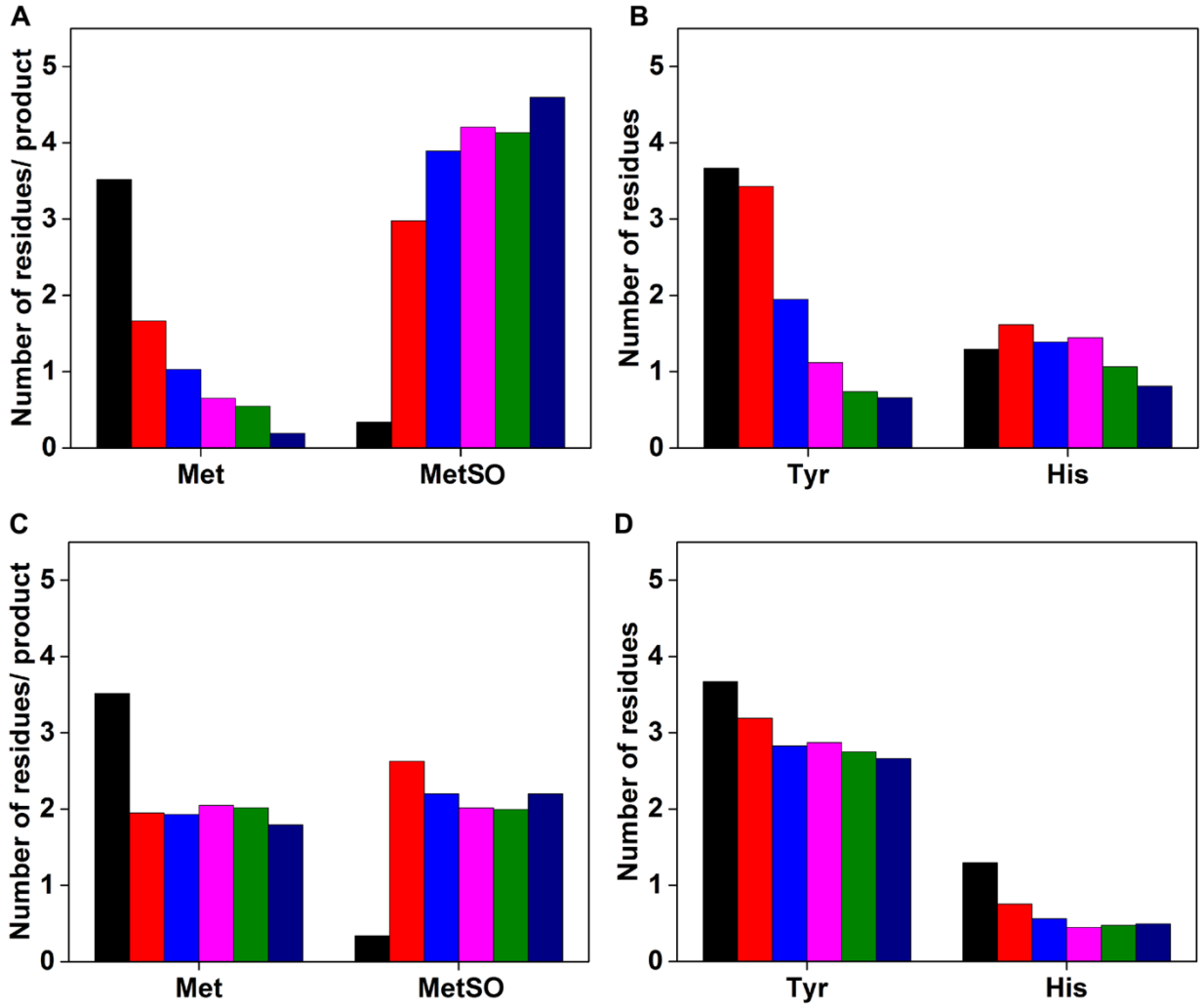

Fig. 3. Changes in composition of Met, Tyr, His and Met sulfoxide on α–SN induced by Cu^{2+}/H_2O_2–mediated oxidation in the absence and presence of $AscH^-$. Bar graphs showing normalized values for the loss of Met, Tyr, His and production of Met sulfoxide. (**A** and **B**) Condition 1 with molar ratio of 1:2.3:7.8:0 between α–SN : Cu^{2+} : H_2O_2. (**C** and **D**) Condition 5 with molar ratio of 1:2.3:7.8:7.8 between α–SN: Cu^{2+}: H_2O_2: $AscH^-$. Data shown are for five–time points 0.1 min (red), 5 min (blue), 15 min (pink), 60 min (green), and 360 min (navy blue), whereas black color bar represents composition of respective residues and Met sulfoxide in the native α–SN; for details, see Materials and methods. Except for 0.1 min sample, all other reaction mixtures were incubated at 37 °C for the time intervals indicated.

Running title: Copper-ion catalyzed oxidation of α-synuclein

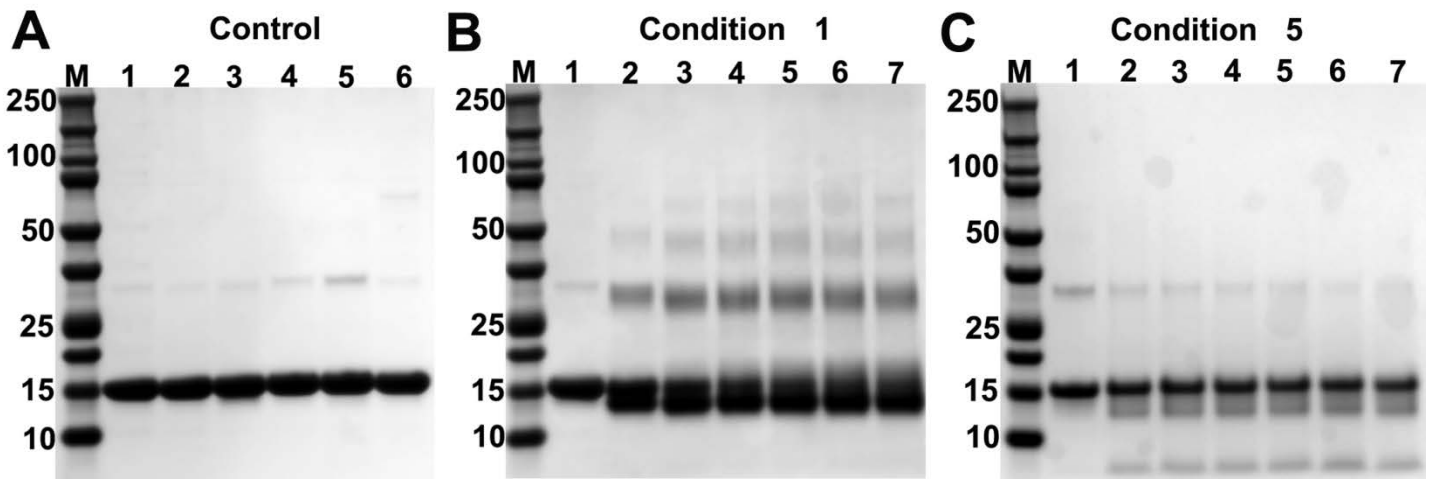

Fig. 4. SDS–PAGE analyses of control and oxidized α–SN exposed to various concentrations of Cu^{2+} and H_2O_2, without and with $AscH^-$. Samples were prepared as indicated in the Materials and methods. (**A**) Control samples; lane M, molecular mass markers; lane – 1, native α–SN; lane – 2, α–SN incubated at 37 °C for 360 min; lane – 3, α–SN incubated with Cu^{2+} at 37 °C for 360 min; lane – 4, α–SN incubated with H_2O_2 at 37 °C for 360 min; lane – 5, α–SN incubated with $AscH^-$ at 37 °C for 360 min; lane – 6, α–SN incubated with EDTA at 37 °C for 360 min. (**B**) Oxidation with condition 1, and (**C**) oxidation with condition 5 with the following samples: lane M, molecular mass markers; lane – 1, oxidation for 0.1 min; lane – 2, oxidation for 5 min; lane – 3, oxidation for 15 min; lane – 4, oxidation for 30 min; lane – 5, oxidation for 60 min; lane – 6, oxidation for 180 min; lane – 7, oxidation for 360 min.

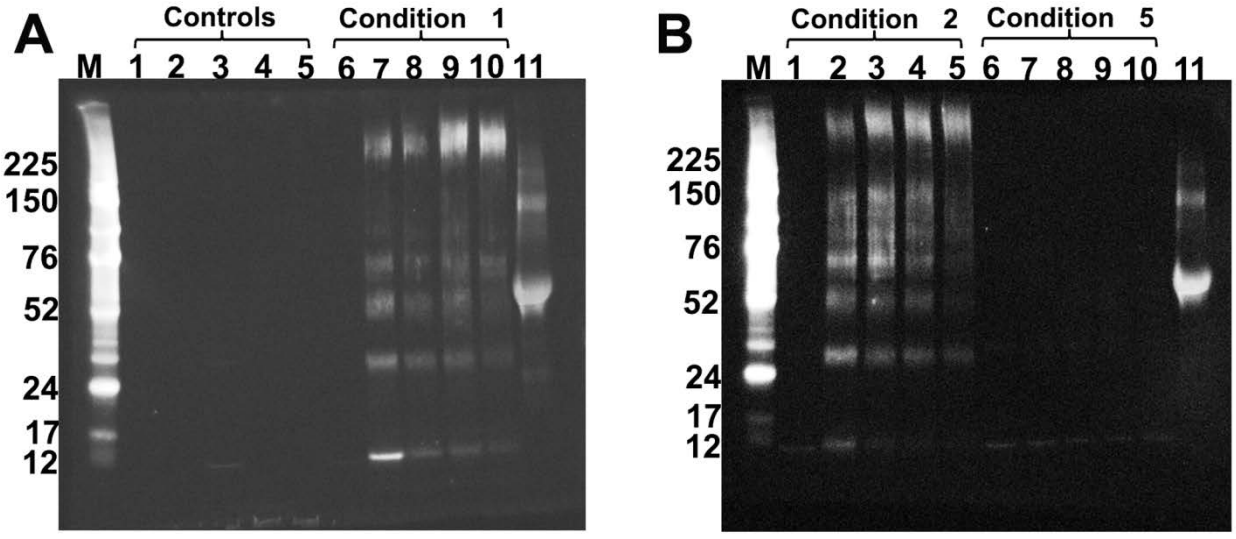

Fig. 5. Detection of dityrosine on oxidized α–SN by Western–blotting. Oxidized α–SN samples (22μM) were electrophoresed and transferred to nitrocellulose membranes as described in the Materials and methods. (**A**) Controls organized as follows; lane M – molecular mass markers; lane – 1, native α–SN; lane – 2, α–SN incubated at 37 °C for 360 min; lane – 3, α–SN incubated with Cu^{2+} at 37 °C for 360 min; lane – 4, α–SN incubated with H_2O_2 at 37 °C for 360 min; lane – 5, α–SN incubated with $AscH^-$ at 37 °C for 360 min. Lanes 6 – 10 are samples of α–SN oxidized under condition 1 for 0.1 min, 5, 15, 60 and 360 min, respectively. (**B**) Lanes 1–5: as lanes 6–10 of (a) except with oxidation under condition 2 (higher Cu^{2+} concentration) for 0.1 min, 5, 15, 60 and 360 min. Lanes 6–10: with oxidation under condition 5 (presence of $AscH^-$) and oxidation for 0.1 min, 5, 15, 60 and 360 min. Lane 11 in both images is a positive control consisting of 3 mg mL^{-1} glucose–6–phosphate dehydrogenase exposed to $^1O_2$ generated using 10 μM Rose Bengal and visible light, for 90 min at 4°C [48].

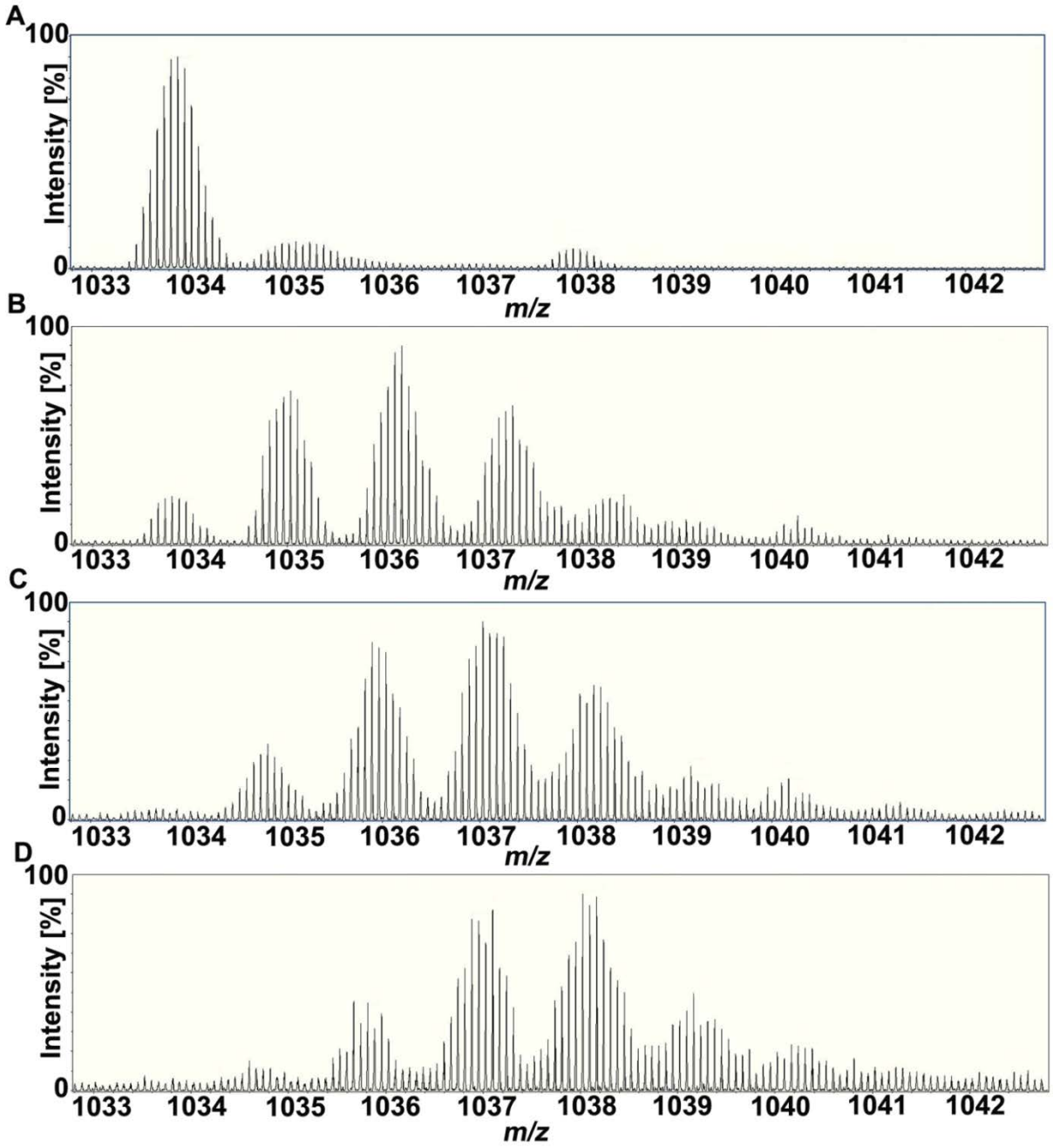

Fig. 6. Positive ion ESI–MS spectra of Cu^{2+}/H_2O_2–oxidized α–SN in the absence of $AscH^-$ (condition 1) with using molar ratios of 1:2.3:7.8 for α– SN: Cu^{2+}: H_2O_2. (**A**) Native α–SN, (**B**) oxidized for 0.1 min, (**C**) oxidized for 5 min and, (**D**) oxidized for 15 min. The *m/z* values indicated are monoisotopic masses.

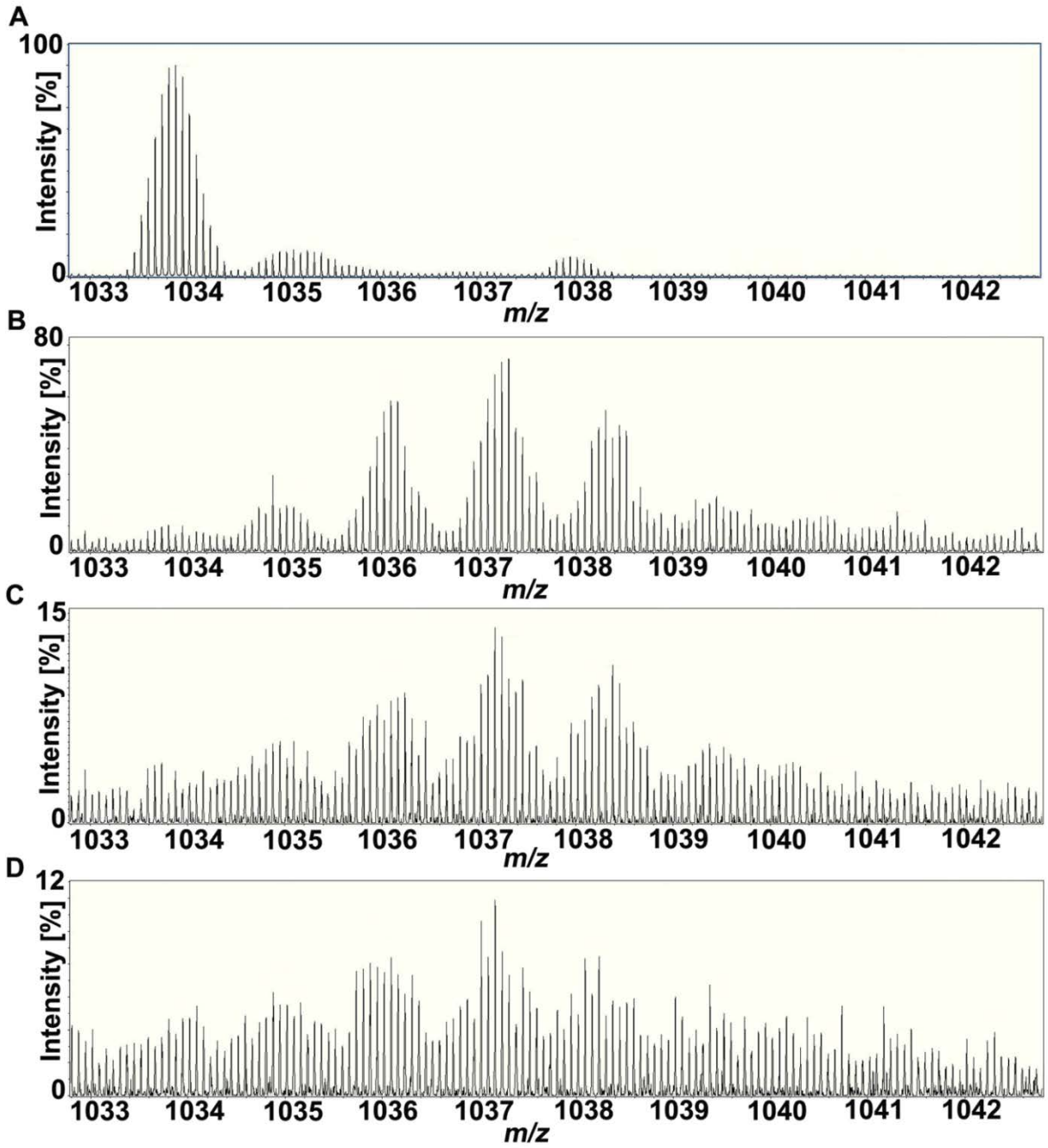

Fig. 7. Positive ion ESI–MS spectra of Cu^{2+}/H_2O_2–oxidized α–SN in the presence of $AscH^-$ (condition 5) using molar ratios of 1:2.3:7.8:7.8 between α– SN: Cu^{2+}: H_2O_2: $AscH^-$. (**A**) Native α–SN, (**B**) oxidized for 0.1 min, (**C**) oxidized for 5 min and, (**D**) oxidized for 15 min. The *m/z* values indicated are monoisotopic masses.

Running title: Copper-ion catalyzed oxidation of α-synuclein

Table 1: Concentrations and molar ratios of reagents employed to initiate oxidation of α–SN.

Samples	Final concentrations in reaction mixture (μM)				Molar ratios
	α–SN	**$CuCl_2$**	**H_2O_2**	**$AscH^-$**	**(α–SN: Cu^{2+}: H_2O_2: $AscH^-$)**
Condition 1	57.6	135	450	0	1:2.3:7.8:0
Condition 2	57.6	270	450	0	1:4.7:7.8:0
Condition 3	57.6	135	900	0	1:2.3:15.6:0
Condition 4	57.6	270	900	0	1:4.7:15.6:0
Condition 5	57.6	135	450	450	1:2.3:7.8:7.8
Condition 6	57.6	270	900	900	1:4.7:15.6:15.6

Reaction set–up for five control samples at two-time intervals (0.1 min and 360 min) are described in Table S2.

2 mM EDTA was added to terminate the MCO reaction after each time interval as described in the Materials and methods.

References:

[1] J.K. Andersen, Oxidative stress in neurodegeneration: cause or consequence?, Nat Med 10 Suppl (2004) S18-25.

[2] K.J. Barnham, C.L. Masters, A.I. Bush, Neurodegenerative diseases and oxidative stress, Nat Rev Drug Discov 3(3) (2004) 205-14.

[3] B.C. Dickinson, C.J. Chang, Chemistry and biology of reactive oxygen species in signaling or stress responses, Nat Chem Biol 7(8) (2011) 504-11.

[4] C. Nathan, A. Cunningham-Bussel, Beyond oxidative stress: an immunologist's guide to reactive oxygen species, Nat Rev Immunol 13(5) (2013) 349-61.

[5] M.J. Davies, Protein oxidation and peroxidation, Biochem J 473(7) (2016) 805-25.

[6] B.I. Giasson, J.E. Duda, I.V. Murray, Q. Chen, J.M. Souza, H.I. Hurtig, H. Ischiropoulos, J.Q. Trojanowski, V.M. Lee, Oxidative damage linked to neurodegeneration by selective alpha-synuclein nitration in synucleinopathy lesions, Science 290(5493) (2000) 985-9.

[7] D.A. Butterfield, Amyloid β-peptide [1-42]-associated free radical-induced oxidative stress and neurodegeneration in Alzheimer's disease brain: mechanisms and consequences, Curr Med Chem 10(24) (2003) 2651-9.

[8] M.K. Tiwari, K.P. Kepp, β-Amyloid pathogenesis: Chemical properties versus cellular levels, Alzheimers Dement 12(2) (2016) 184-194.

[9] R.J. Ferrante, S.E. Browne, L.A. Shinobu, A.C. Bowling, M.J. Baik, U. MacGarvey, N.W. Kowall, R.H. Brown, M.F. Beal, Evidence of Increased Oxidative Damage in Both Sporadic and Familial Amyotrophic Lateral Sclerosis, J Neurochem 69(5) (1997) 2064-2074.

[10] J. Gil-Mohapel, P.S. Brocardo, B.R. Christie, The role of oxidative stress in Huntington's disease: are antioxidants good therapeutic candidates?, Curr Drug Targets 15(4) (2014) 454-68.

[11] M. Guentchev, T. VoigtlÃ¤nder, C. Haberler, M.H. Groschup, H. Budka, Evidence for Oxidative Stress in Experimental Prion Disease, Neurobiol Dis 7(4) (2000) 270-273.

[12] S. Gandhi, N.W. Wood, Genome-wide association studies: the key to unlocking neurodegeneration?, Nat Neurosci 13(7) (2010) 789-94.

[13] C. Henchcliffe, M.F. Beal, Mitochondrial biology and oxidative stress in Parkinson disease pathogenesis, Nat Clin Pract Neurol 4(11) (2008) 600-9.

[14] S. Papapetropoulos, N. Adi, J. Ellul, A.A. Argyriou, E. Chroni, A prospective study of familial versus sporadic Parkinson's disease, Neurodegener Dis 4(6) (2007) 424-7.

[15] M.G. Spillantini, R.A. Crowther, R. Jakes, N.J. Cairns, P.L. Lantos, M. Goedert, Filamentous α-Synuclein inclusions link multiple system atrophy with Parkinson's disease and dementia with Lewy bodies, Neurosci Lett 251(3) (1998) 205-8.

[16] M.G. Spillantini, R.A. Crowther, R. Jakes, M. Hasegawa, M. Goedert, α-Synuclein in filamentous inclusions of Lewy bodies from Parkinson's disease and dementia with lewy bodies, Proc Natl Acad Sci U S A 95(11) (1998) 6469-73.

[17] L. Maroteaux, J.T. Campanelli, R.H. Scheller, Synuclein: a neuron-specific protein localized to the nucleus and presynaptic nerve terminal, J Neurosci 8(8) (1988) 2804-15.

[18] T. Yasuda, Y. Nakata, H. Mochizuki, α-Synuclein and neuronal cell death, Mol Neurobiol 47(2) (2013) 466-83.

[19] O. Marques, T.F. Outeiro, Alpha-synuclein: from secretion to dysfunction and death, Cell Death Dis 3 (2012) e350.

[20] V.N. Uversky, J. Li, A.L. Fink, Evidence for a partially folded intermediate in α-Synuclein fibril formation, J Biol Chem 276(14) (2001) 10737-44.

[21] P.P. Michel, E.C. Hirsch, S. Hunot, Understanding Dopaminergic Cell Death Pathways in Parkinson Disease, Neuron 90(4) (2016) 675-91.

[22] A. Umeno, V. Biju, Y. Yoshida, In vivo ROS production and use of oxidative stress-derived biomarkers to detect the onset of diseases such as Alzheimer's disease, Parkinson's disease, and diabetes, Free Radic Res 51(4) (2017) 413-427.

[23] C. Zhou, Y. Huang, S. Przedborski, Oxidative stress in Parkinson's disease: a mechanism of pathogenic and therapeutic significance, Ann N Y Acad Sci 1147 (2008) 93-104.

[24] V.N. Uversky, G. Yamin, P.O. Souillac, J. Goers, C.B. Glaser, A.L. Fink, Methionine oxidation inhibits fibrillation of human α-Synuclein in vitro, FEBS Lett 517(1-3) (2002) 239-44.

[25] J.M. Souza, B.I. Giasson, Q. Chen, V.M. Lee, H. Ischiropoulos, Dityrosine cross-linking promotes formation of stable α-synuclein polymers. Implication of nitrative and oxidative stress in the pathogenesis of neurodegenerative synucleinopathies, J Biol Chem 275(24) (2000) 18344-9.

[26] Y.K. Al-Hilaly, L. Biasetti, B.J. Blakeman, S.J. Pollack, S. Zibaee, A. Abdul-Sada, J.R. Thorpe, W.F. Xue, L.C. Serpell, The involvement of dityrosine crosslinking in α-synuclein assembly and deposition in Lewy Bodies in Parkinson's disease, Sci Rep 6 (2016) 39171.

[27] D.T. Dexter, A. Carayon, F. Javoy-Agid, Y. Agid, F.R. Wells, S.E. Daniel, A.J. Lees, P. Jenner, C.D. Marsden, Alterations in the levels of iron, ferritin and other trace metals in Parkinson's disease and other neurodegenerative diseases affecting the basal ganglia, Brain 114 (Pt 4) (1991) 1953-75.

[28] D.T. Dexter, F.R. Wells, A.J. Lees, F. Agid, Y. Agid, P. Jenner, C.D. Marsden, Increased nigral iron content and alterations in other metal ions occurring in brain in Parkinson's disease, J Neurochem 52(6) (1989) 1830-6.

[29] H.S. Pall, A.C. Williams, D.R. Blake, J. Lunec, J.M. Gutteridge, M. Hall, A. Taylor, Raised cerebrospinal-fluid copper concentration in Parkinson's disease, Lancet 2(8553) (1987) 238-41.

[30] K.J. Barnham, A.I. Bush, Biological metals and metal-targeting compounds in major neurodegenerative diseases, Chem Soc Rev 43(19) (2014) 6727-49.

[31] G. Yamin, C.B. Glaser, V.N. Uversky, A.L. Fink, Certain metals trigger fibrillation of methionine-oxidized α-synuclein, J Biol Chem 278(30) (2003) 27630-5.

[32] R.M. Rasia, C.W. Bertoncini, D. Marsh, W. Hoyer, D. Cherny, M. Zweckstetter, C. Griesinger, T.M. Jovin, C.O. Fernandez, Structural characterization of copper(II) binding to α-synuclein: Insights into the bioinorganic chemistry of Parkinson's disease, Proc Natl Acad Sci U S A 102(12) (2005) 4294-9.

[33] T.S. Ulmer, A. Bax, Comparison of structure and dynamics of micelle-bound human α-synuclein and Parkinson disease variants, J Biol Chem 280(52) (2005) 43179-87.

[34] L. Breydo, J.W. Wu, V.N. Uversky, α-Synuclein misfolding and Parkinson's disease, Biochim Biophys Acta 1822(2) (2012) 261-85.

[35] J.C. Lee, H.B. Gray, J.R. Winkler, Copper(II) binding to α-synuclein, the Parkinson's protein, J Am Chem Soc 130(22) (2008) 6898-9.

[36] O. Tavassoly, S. Nokhrin, O.Y. Dmitriev, J.S. Lee, Cu(II) and dopamine bind to α-synuclein and cause large conformational changes, FEBS J 281(12) (2013) 2738-53.

[37] S.C. Drew, S.L. Leong, C.L. Pham, D.J. Tew, C.L. Masters, L.A. Miles, R. Cappai, K.J. Barnham, Cu^{2+} binding modes of recombinant α-synuclein - insights from EPR spectroscopy, J Am Chem Soc 130(24) (2008) 7766-73.

[38] N.B. Cole, D.D. Murphy, J. Lebowitz, L. Di Noto, R.L. Levine, R.L. Nussbaum, Metal-catalyzed oxidation of α-Synuclein: helping to define the relationship between oligomers, protofibrils, and filaments, J Biol Chem 280(10) (2005) 9678-90.

[39] S.R. Paik, H.J. Shin, J.H. Lee, Metal-catalyzed oxidation of α-Synuclein in the presence of Copper(II) and hydrogen peroxide, Arch Biochem Biophys 378(2) (2000) 269-77.

[40] S.R. Paik, H.J. Shin, J.H. Lee, C.S. Chang, J. Kim, Copper(II)-induced self-oligomerization of α-Synuclein, Biochem J 340 (Pt 3) (1999) 821-8.

[41] V.N. Uversky, J. Li, A.L. Fink, Metal-triggered structural transformations, aggregation, and fibrillation of human α-Synuclein. A possible molecular NK between Parkinson's disease and heavy metal exposure, J Biol Chem 276(47) (2001) 44284-96.

[42] G. Zhao, N.D. Chasteen, Oxidation of Good's buffers by hydrogen peroxide, Anal Biochem 349(2) (2006) 262-7.

[43] C. Sahin, N. Lorenzen, L. Lemminger, G. Christiansen, I.M. Møller, L.B. Vesterager, L.O. Pedersen, K. Fog, P. Kallunki, D.E. Otzen, Antibodies against the C-terminus of α-synuclein modulate its fibrillation, Biophys Chem 220 (2017) 34-41.

[44] R.F. Beers, Jr., I.W. Sizer, A spectrophotometric method for measuring the breakdown of hydrogen peroxide by catalase, J Biol Chem 195(1) (1952) 133-40.

[45] L. Bousset, L. Pieri, G. Ruiz-Arlandis, J. Gath, P.H. Jensen, B. Habenstein, K. Madiona, V. Olieric, A. Bockmann, B.H. Meier, R. Melki, Structural and functional characterization of two alpha-synuclein strains, Nat Commun 4 (2013) 2575.

[46] B. Rey, C. Degletagne, J. Bodennec, P.A. Monternier, M. Mortz, D. Roussel, C. Romestaing, J.L. Rouanet, J. Tornos, C. Duchamp, Hormetic response triggers multifaceted anti-oxidant strategies in immature king penguins (*Aptenodytes patagonicus*), Free Radic Biol Med 97 (2016) 577-587.

[47] P.K. Smith, R.I. Krohn, G.T. Hermanson, A.K. Mallia, F.H. Gartner, M.D. Provenzano, E.K. Fujimoto, N.M. Goeke, B.J. Olson, D.C. Klenk, Measurement of protein using bicinchoninic acid, Anal Biochem 150(1) (1985) 76-85.

[48] F. Leinisch, M. Mariotti, M. Rykaer, C. Lopez-Alarcon, P. Hagglund, M.J. Davies, Peroxyl radical- and photo-oxidation of glucose 6-phosphate dehydrogenase generates cross-links and functional changes via oxidation of tyrosine and tryptophan residues, Free Radic Biol Med 112 (2017) 240-252.

[49] A.C. Kramer, P.W. Thulstrup, M.N. Lund, M.J. Davies, Key role of cysteine residues and sulfenic acids in thermal- and H_2O_2-mediated modification of β-lactoglobulin, Free Radic Biol Med 97 (2016) 544-555.

[50] A. Iyer, S.J. Roeters, N. Schilderink, B. Hommersom, R.M. Heeren, S. Woutersen, M.M. Claessens, V. Subramaniam, The impact of N-terminal acetylation of α-synuclein on phospholipid membrane binding and fibril structure, J Biol Chem 291(40) (2016) 21110-21122.

[51] A. Iwai, E. Masliah, M. Yoshimoto, N. Ge, L. Flanagan, H.A. de Silva, A. Kittel, T. Saitoh, The precursor protein of non-Aβ component of Alzheimer's disease amyloid is a presynaptic protein of the central nervous system, Neuron 14(2) (1995) 467-75.

[52] A. Hopt, S. Korte, H. Fink, U. Panne, R. Niessner, R. Jahn, H. Kretzschmar, J. Herms, Methods for studying synaptosomal copper release, J Neurosci Methods 128(1-2) (2003) 159-72.

[53] M.L. Schlief, J.D. Gitlin, Copper homeostasis in the CNS: a novel link between the NMDA receptor and copper homeostasis in the hippocampus, Mol Neurobiol 33(2) (2006) 81-90.

[54] E.R. Stadtman, C.N. Oliver, Metal-catalyzed oxidation of proteins. Physiological consequences, J Biol Chem 266(4) (1991) 2005-8.

[55] C. Wang, L. Liu, L. Zhang, Y. Peng, F. Zhou, Redox reactions of the α-synuclein−Cu^{2+} complex and their effects on neuronal cell viability, Biochemistry 49(37) 8134-8142.

[56] J. Yin, J.W. Chu, M.S. Ricci, D.N. Brems, D.I. Wang, B.L. Trout, Effects of antioxidants on the hydrogen peroxide-mediated oxidation of methionine residues in granulocyte colony-stimulating factor and human parathyroid hormone fragment 13-34, Pharm Res 21(12) (2004) 2377-83.

[57] W.J. Ma, E.H. Cao, J.F. Qin, The involvement of singlet oxygen in copper-phenanthroline/H2O2-induced DNA base damage: a chemiluminescent study, Redox Rep 4(6) (1999) 271-276.

[58] T. Ookawara, N. Kawamura, Y. Kitagawa, N. Taniguchi, Site-specific and random fragmentation of Cu,Zn-superoxide dismutase by glycation reaction. Implication of reactive oxygen species, J Biol Chem 267(26) (1992) 18505-10.

[59] W.J. Ferguson, K.I. Braunschweiger, W.R. Braunschweiger, J.R. Smith, J.J. McCormick, C.C. Wasmann, N.P. Jarvis, D.H. Bell, N.E. Good, Hydrogen ion buffers for biological research, Anal Biochem 104(2) (1980) 300-10.

[60] S. Stepanova, V. Kasicka, Recent applications of capillary electromigration methods to separation and analysis of proteins, Anal Chim Acta 933 (2016) 23-42.

[61] J. Stocks, N.E. Miller, Capillary electrophoresis to monitor the oxidative modification of low density lipoproteins, J Lipid Res 39(6) (1998) 1305-9.

[62] D. Weber, M.J. Davies, T. Grune, Determination of protein carbonyls in plasma, cell extracts, tissue homogenates, isolated proteins: Focus on sample preparation and derivatization conditions, Redox Biol 5 (2015) 367-80.

[63] S.B. Nimse, D. Pal, Free radicals, natural antioxidants, and their reaction mechanisms, RSC Adv 5(35) (2015) 27986-28006.

[64] B.M. Hoey, J. Butler, The repair of oxidized amino acids by antioxidants, Biochim Biophys Acta 791(2) (1984) 212-8.

[65] J.C. Mayo, D.X. Tan, R.M. Sainz, M. Natarajan, S. Lopez-Burillo, R.J. Reiter, Protection against oxidative protein damage induced by metal-catalyzed reaction or alkylperoxyl radicals: comparative effects of melatonin and other antioxidants, Biochim Biophys Acta 1620(1) (2003) 139-150.

[66] Q. Yuan, X. Zhu, L.M. Sayre, Chemical nature of stochastic generation of protein-based carbonyls: metal-catalyzed oxidation versus modification by products of lipid oxidation, Chem Res Toxicol 20(1) (2007) 129-39.

[67] V.M. Monnier, I. Nemet, D.R. Sell, M.F. Weiss, Transition metals and other forms of oxidative protein damage in renal disease, in: T. Miyata, K.-U. Eckardt, M. Nangaku (Eds.), Studies on Renal Disorders, Humana Press, Totowa, NJ, 2011, pp. 25-50.

[68] I.M. Møller, A. Rogowska-Wrzesinska, R.S. Rao, Protein carbonylation and metal-catalyzed protein oxidation in a cellular perspective, J Proteomics 74(11) (2011) 2228-42.

[69] R.J. Mason, A.R. Paskins, C.F. Dalton, D.P. Smith, Copper binding and subsequent aggregation of α-synuclein are modulated by N-terminal acetylation and ablated by the H50Q missense mutation, Biochemistry 55(34) (2016) 4737-41.

[70] A. Binolfi, A. Limatola, S. Verzini, J. Kosten, F.X. Theillet, H.M. Rose, B. Bekei, M. Stuiver, M. van Rossum, P. Selenko, Intracellular repair of oxidation-damaged α-synuclein fails to target C-terminal modification sites, Nat Commun 7 (2016) 10251.

[71] C.G. Dudzik, E.D. Walter, G.L. Millhauser, Coordination features and affinity of the Cu^{2+} site in the α-synuclein protein of Parkinson's disease, Biochemistry 50(11) (2011) 1771-7.

[72] M.J. Davies, The oxidative environment and protein damage, Biochim Biophys Acta 1703(2) (2005) 93-109.

[73] S.H. Gellman, On the role of methionine residues in the sequence-independent recognition of nonpolar protein surfaces, Biochemistry 30(27) (1991) 6633-6.

[74] W. Zhou, C. Long, S.H. Reaney, D.A. Di Monte, A.L. Fink, V.N. Uversky, Methionine oxidation stabilizes non-toxic oligomers of α-synuclein through strengthening the auto-inhibitory intra-molecular long-range interactions, Biochim Biophys Acta 1802(3) (2010) 322-30.

[75] G.R. Buettner, B.A. Jurkiewicz, Catalytic metals, ascorbate and free radicals: combinations to avoid, Radiat Res 145(5) (1996) 532-41.

[76] C. Cheignon, F. Collin, P. Faller, C. Hureau, Is ascorbate Dr Jekyll or Mr Hyde in the Cu(Aβ) mediated oxidative stress linked to Alzheimer's disease?, Dalton Trans 45(32) (2016) 12627-12631.

[77] T. Hoshi, S. Heinemann, Regulation of cell function by methionine oxidation and reduction, J Physiol 531(Pt 1) (2001) 1-11.

[78] V. Kadlcik, C. Sicard-Roselli, T.A. Mattioli, M. Kodicek, C. Houée-Levin, One-electron oxidation of β-amyloid peptide: sequence modulation of reactivity, Free Radic Biol Med 37(6) (2004) 881-891.

[79] C. Schoneich, D. Pogocki, G.L. Hug, K. Bobrowski, Free radical reactions of methionine in peptides: mechanisms relevant to β-amyloid oxidation and Alzheimer's disease, J Am Chem Soc 125(45) (2003) 13700-13.

[80] A. Binolfi, L. Quintanar, C.W. Bertoncini, C. Griesinger, C.O. Fernández, Bioinorganic chemistry of copper coordination to alpha-synuclein: Relevance to Parkinson's disease, Coord Chem Rev 256(19) (2012) 2188-2201.

[81] Y.C. Chi, G.S. Armstrong, D.N. Jones, E.Z. Eisenmesser, C.W. Liu, Residue histidine 50 plays a key role in protecting alpha-synuclein from aggregation at physiological pH, J Biol Chem 289(22) (2014) 15474-81.

[82] B.E. Sturgeon, H.J. Sipe, Jr., D.P. Barr, J.T. Corbett, J.G. Martinez, R.P. Mason, The fate of the oxidizing tyrosyl radical in the presence of glutathione and ascorbate. Implications for the radical sink hypothesis, J Biol Chem 273(46) (1998) 30116-21.

[83] L.K. Folkes, M. Trujillo, S. Bartesaghi, R. Radi, P. Wardman, Kinetics of reduction of tyrosine phenoxyl radicals by glutathione, Arch Biochem Biophys 506(2) (2011) 242-9.

[84] N. Bengoa-Vergniory, R.F. Roberts, R. Wade-Martins, J. Alegre-Abarrategui, Alpha-synuclein oligomers: a new hope, Acta Neuropathol 134(6) (2017) 819-838.

[85] M. Ingelsson, Alpha-Synuclein oligomers-neurotoxic molecules in Parkinson's disease and other Lewy body disorders, Front Neurosci 10 (2016) 408.

[86] A.L. Fink, The aggregation and fibrillation of α-synuclein, Acc Chem Res 39(9) (2006) 628-34.

[87] B. Alvarez-Castelao, M. Goethals, J. Vandekerckhove, J.G. Castano, Mechanism of cleavage of alpha-synuclein by the 20S proteasome and modulation of its degradation by the RedOx state of the N-terminal methionines, Biochim Biophys Acta 1843(2) (2014) 352-65.

[88] A.S. Maltsev, J. Chen, R.L. Levine, A. Bax, Site-specific interaction between α-Synuclein and membranes probed by NMR-observed methionine oxidation rates, , J Am Chem Soc 135(8) (2013) 2943-2946.

[89] S.L. Leong, C.L. Pham, D. Galatis, M.T. Fodero-Tavoletti, K. Perez, A.F. Hill, C.L. Masters, F.E. Ali, K.J. Barnham, R. Cappai, Formation of dopamine-mediated alpha-synuclein-soluble oligomers requires methionine oxidation, Free Radic Biol Med 46(10) (2009) 1328-37.

[90] L. Chen, M. Periquet, X. Wang, A. Negro, P.J. McLean, B.T. Hyman, M.B. Feany, Tyrosine and serine phosphorylation of α-synuclein have opposing effects on neurotoxicity and soluble oligomer formation, J Clin Invest 119(11) (2009) 3257-3265.

[91] B. Winner, R. Jappelli, S.K. Maji, P.A. Desplats, L. Boyer, S. Aigner, C. Hetzer, T. Loher, M. Vilar, S. Campioni, C. Tzitzilonis, A. Soragni, S. Jessberger, H. Mira, A. Consiglio, E. Pham, E. Masliah, F.H. Gage, R. Riek, In vivo demonstration that α-synuclein oligomers are toxic, Proc Natl Acad Sci USA 108(10) (2011) 4194-4199.

[92] S. Krishnan, E.Y. Chi, S.J. Wood, B.S. Kendrick, C. Li, W. Garzon-Rodriguez, J. Wypych, T.W. Randolph, L.O. Narhi, A.L. Biere, M. Citron, J.F. Carpenter, Oxidative dimer formation is the critical rate-limiting step for Parkinson's disease α-Synuclein fibrillogenesis, Biochemistry 42(3) (2003) 829-837.

[93] J. Du, J.J. Cullen, G.R. Buettner, Ascorbic acid: chemistry, biology and the treatment of cancer, Biochim Biophys Acta 1826(2) (2012) 443-57.

[94] A.S. Domazou, W.H. Koppenol, J.M. Gebicki, Efficient repair of protein radicals by ascorbate, Free Radic Biol Med 46(8) (2009) 1049-57.

[95] W. Vogt, Oxidation of methionyl residues in proteins: tools, targets, and reversal, Free Radic Biol Med 18(1) (1995) 93-105.

[96] T. Nauser, J. Pelling, C. Schöneich, Thiyl radical reaction with amino acid side chains: rate constants for hydrogen transfer and relevance for posttranslational protein modification, Chem Res Toxicol 17(10) (2004) 1323-1328.

[97] A. Binolfi, E.E. Rodriguez, D. Valensin, N. D'Amelio, E. Ippoliti, G. Obal, R. Duran, A. Magistrato, O. Pritsch, M. Zweckstetter, G. Valensin, P. Carloni, L. Quintanar, C. Griesinger, C.O. Fernández, Bioinorganic chemistry of Parkinson's disease: structural determinants for the copper-mediated amyloid formation of alpha-synuclein, Inorganic Chemistry 49(22) (2010) 10668-10679.

[98] W.A. Prutz, J. Butler, E.J. Land, Phenol coupling initiated by one-electron oxidation of tyrosine units in peptides and histone, Int J Radiat Biol Relat Stud Phys Chem Med 44(2) (1983) 183-96.

[99] Y. Kato, N. Kitamoto, Y. Kawai, T. Osawa, The hydrogen peroxide/copper ion system, but not other metal-catalyzed oxidation systems, produces protein-bound dityrosine, Free Radic Biol Med 31(5) (2001) 624-632.

[100] J.M. Gebicki, T. Nauser, A. Domazou, D. Steinmann, P.L. Bounds, W.H. Koppenol, Reduction of protein radicals by GSH and ascorbate: potential biological significance, Amino Acids 39(5) (2010) 1131-7.